*horticulturae*

MDPI

*Article*

# Physiological Responses of Highbush Blueberry (*Vaccinium corymbosum* L.) to Combined Water Deficit and Aluminum Stress: The Role of Methyl Jasmonate in Enhancing Stress Resistance

**Jhonny Quintana [1,2], Cristina Cáceres [3], Jéssica Costa [2,4], Cledir Santos [4,5], Jorge Gonzalez-Villagra [6], Claudio Inostroza-Blancheteau [7,8], Adriano Nunes-Nesi [9] and Marjorie Reyes-Díaz [2,4,*]**

1 Programa de Doctorado en Ciencias Mención en Biología Celular y Molecular Aplicada, Universidad de La Frontera, Temuco P.O. Box 54-D, Chile; j.quintana06@ufromail.cl
2 Laboratorio de Ecofisiología Molecular y Funcional de Plantas, Departamento de Ciencias Químicas y Recursos Naturales, Facultad de Ingeniería y Ciencias, Universidad de La Frontera, Temuco P.O. Box 54-D, Chile; jessica.costa@ufrontera.cl
3 Programa de Doctorado en Ciencias de Recursos Naturales, Universidad de La Frontera, Temuco 4811230, Chile; c.caceres02@ufromail.cl
4 Center of Plant, Soil Interaction and Natural Resources Biotechnology, Scientific and Technological Bioresource Nucleus (BIOREN-UFRO), Universidad de La Frontera, Temuco P.O. Box 54-D, Chile; cledir.santos@ufrontera.cl
5 Postgraduate Program in Biotechnology, Federal University of Technology-Paraná, Ponta Grossa 84017-220, Brazil
6 Escuela de Agronomía, Facultad de Ciencias, Ingeniería y Tecnología, Universidad Mayor, Temuco 4780000, Chile; jorge.gonzalez@umayor.cl
7 Laboratorio de Fisiología y Biotecnología Vegetal, Departamento de Ciencias Agropecuarias y Acuícolas, Facultad de Recursos Naturales, Universidad Católica de Temuco, Temuco P.O. Box 15-D, Chile; claudio.inostroza@uct.cl
8 ANID-Millenium Science Initiative Program-Millenium Nucleus in Data Science for Plant Resilience (Phytolearning), Santiago 8370186, Chile
9 National Institute of Science and Technology on Plant Physiology Under Stress Conditions, Departamento de Biologia Vegetal, Universidade Federal de Viçosa, Viçosa 36570-900, Brazil; nunesnesi@ufv.br
* Correspondence: marjorie.reyes@ufrontera.cl

## Abstract

Highbush blueberry (*Vaccinium corymbosum* L.) is widely cultivated in southern Chile on acidic Andisols, where aluminum ($Al^{3+}$) toxicity and water deficit frequently occur simultaneously and limit plant performance. However, the integrated physiological responses to these stresses and the potential protective role of methyl jasmonate (MeJA) remain poorly understood. This study evaluated the physiological, biochemical, and hormonal responses of two cultivars with contrasting resistance, Legacy (Al-resistant) and Star (Al-sensitive), exposed to $Al^{3+}$ stress, water deficit, and their combination, with or without MeJA application. Plants were grown in Andisol ~~soil~~ under greenhouse conditions and subjected to eight treatments, with measurements performed at 7, 14, and 21 days. Exposure to stress conditions resulted in decreased growth, reduced leaf water status, diminished photosynthetic performance, lower pigment stability, and decreased auxin concentration as estimated by Salkowski-reactive indolic compounds. Conversely, stress conditions led to increased aluminum (Al) accumulation, elevated proline levels, enhanced lipid peroxidation, and heightened antioxidant responses. Water deficit produced the strongest reductions in photosynthesis, about 48% in Legacy and 65% in Star, whereas Al accumulated mainly in the roots of Star (14-fold). The combined stress intensified physiological limitations and oxidative damage, particularly in the Star cultivar (4-fold), which showed stronger



Academic Editor: Hao Liu

Received: 8 April 2026
Revised: 1 June 2026
Accepted: 4 June 2026
Published: 15 June 2026

reductions in photosynthetic parameters, higher Al accumulation, and greater lipid peroxidation. In contrast, Legacy maintained more stable physiological performance. Exogenous MeJA mitigated stress effects by reducing Al accumulation (30–35%) and oxidative damage, improving photosynthetic performance (40–60%) and water status, and partially restoring auxin levels and growth in both cultivars, being more evident in the resistant cultivar Legacy. These results indicate that MeJA contributes to the regulation of physiological and antioxidant responses associated with resistance to combined Al toxicity and water deficit in highbush blueberry.

**Keywords:** Andisols; antioxidant response; gas exchange; oxidative damage; phytohormonal regulation; photosystem II; stress physiology; xanthophyll cycle

## 1. Introduction

Climate change has profoundly affected agricultural systems worldwide, particularly through its impact on water resources distribution and availability [1,2]. Drought represents one of the most severe challenges to agricultural production, causing yield losses of ca. 40–60% in major crops globally [3,4]. In Chile, a prolonged mega-drought that began in 2010 has positioned the country among the most water-stressed regions worldwide. This persistent water deficit (WD) has severely compromised agricultural sustainability by limiting water availability for crop production [3–6].

Water deficit (WD) stress can intensify soil-related constraints, further impairing crop performance, particularly in regions with acidic soils. In southern Chile, agricultural production is largely developed on acidic Andisols (pH $\leq$ 5.5). Under acidic soil conditions, the most abundant and phytotoxic form of Al is the trivalent ionic aluminum ($Al^{3+}$), which can significantly impair plant development [7,8]. As a primary effect, $Al^{3+}$ toxicity interferes with root cell division and elongation. The reduced root growth limits the uptake of water and essential nutrients, including iron (Fe), calcium (Ca), magnesium (Mg), manganese (Mn), potassium (K), phosphorus (P), and nitrogen (N) [7,9]. These root-level constraints subsequently translate into above-ground physiological impairments, particularly affecting photosynthesis. These effects include reduced leaf chlorophyll content, stomatal restrictions, and the inactivation of chloroplast enzymes (e.g., ribulose-1,5-bisphosphate carboxylase/oxygenase—RuBisCO) [10,11]. Furthermore, Al-induced accumulation of reactive oxygen species (ROS) triggers systemic oxidative stress [9,12–14] and disrupts carbohydrate metabolism by inhibiting key enzymes (e.g., α-amylases, β-amylases, and starch phosphorylases) [15]. These soil-related constraints are particularly relevant for perennial fruit crops cultivated in Andisols, such as highbush blueberry (*Vaccinium corymbosum* L.). Andisols are characterized by high concentrations of phytotoxic $Al^{3+}$, which negatively impact plant growth, yield, and fruit quality [16,17]. The combination of abiotic stresses (WD and high $Al^{3+}$ toxicity) can lead to significant crop losses, reducing productivity by up to ca. 50% in various crop species.

Chile remains a key player in the global highbush blueberry (*V. corymbosum* L.) market, with a strong focus on exports to Northern Hemisphere markets during the off-season [18]. In the 2024–2025 season, blueberry exports reached 83,321 tons, increasing an 11% compared with the previous year. The main blueberry production areas extend from the Maule to the La Araucanía regions, with a continued southward expansion of cultivation [18]. In southern Chile, the agricultural systems are predominantly based on Andisols, where phytotoxic $Al^{3+}$ and WD co-exist.

The combined effects of phytotoxic $Al^{3+}$ and WD on *V. corymbosum* plants remain poorly understood. Recent studies have described adaptive strategies of *V. corymbosum* L. under individual abiotic stresses, highlighting the role of primary metabolism and mineral amendments in mitigating $Al^{3+}$ toxicity [19]. Furthermore, exogenous methyl jasmonate (MeJA) has been identified as a key elicitor that protects the photosynthetic apparatus under WD [16] and, under combined toxicity with $Al^{3+}$, can modulate the transcriptional regulation of organic acid transporters and hormonal signaling pathways [17]. Thus, it is also observed that foliar MeJA application induces *ALMT* gene expression in *Solanum lycopersicum* [20] and the expression of *MATE* family genes in *Nicotiana tabacum* [21], which are associated with organic acid exudation as well as Al tolerance and Al detoxification, respectively. Under WD or Al toxicity, MeJA increases chlorophyll and carotenoid accumulation in *Vaccinium corymbosum* and *Impatiens walleriana*, improving photosynthetic efficiency [16,19,22]. Also, the MeJA application under WD showed increased proline and carbohydrate accumulation, playing an important role in osmotic balance to prevent dehydration in *Brassica juncea*, *Ocimum basilicum*, *Glycine max*, and *Fragaria x ananassa* [23–26]. Osmotic regulation is less studied under Al toxicity and even less under combined stresses. Recent studies in highbush blueberry under combined Al toxicity and WD showed an increase in oxidative damage and Al accumulation, provoking a decrease in water potential, photosynthesis, and growth; however, it remains unknown whether this negative effect is due more to $Al^{3+}$ toxicity or more to water deficit, making it important to study not only the combined effect but also the individual effect in the same study.

Despite the advances, integrated knowledge of the interactions among $Al^{3+}$ toxicity, WD, and phytohormonal regulation in fruit crops remains limited. In highbush blueberry, particularly under Andisols conditions, the temporal modulation of oxidative stress, antioxidant defense systems, and hormone-associated responses under combined stresses (e.g., $Al^{3+}$ toxicity and WD) is still poorly documented. Moreover, MeJA has been recognized as an important stress-signaling molecule; however, its role in coordinating antioxidant metabolism, hormonal balance, and physiological performance over time, particularly in cultivars with contrasting tolerance, remains insufficiently explored. Thus, unlike our previous studies [16,17,27], which performed dose screening of MeJA exclusively under combined stress conditions ($Al^{3+}$ toxicity and water deficit), the present study independently evaluates the effects of $Al^{3+}$, water deficit (WD), and their combination (Al + WD) over different time periods, allowing the discrimination of specific responses and synergistic interactions among stress factors. This approach improves mechanistic understanding of how each stressor contributes to physiological damage and enables the development of more precise management strategies tailored to the predominant stress conditions encountered in the field. Therefore, the question arises: how does MeJA alleviate the effects of individual and combined stress through the regulation of auxin concentration as estimated by Salkowski-reactive indolic compounds and/or the antioxidant system?. To address this knowledge gap, the present study aims to evaluate the role of MeJA in modulating the physiological performance, oxidative stress responses, and auxin concentrations of two highbush blueberry cultivars (*V. corymbosum* L. cultivars Legacy and Star) with contrasting tolerance when exposed to $Al^{3+}$ toxicity, WD, and their combined effects under Andisols conditions. By comparing single and combined-stress scenarios, this study provides insights into MeJA-mediated tolerance mechanisms that mitigate $Al^{3+}$- and WD-related constraints in Andisols.

## 2. Materials and Methods

### *2.1. Plant Material and Growth Conditions*

Two blueberry cultivars (*Vaccinium corymbosum* L.) with contrasting Al resistance were used, with Legacy as Al resistant, and Star as Al sensitive [13,19]. The experiment was conducted in a greenhouse at the Universidad de La Frontera (Temuco, Chile). Healthy plants of uniform size were selected and acclimatized at an average temperature of 25 ± 2 °C, a relative air humidity of 70%, and a photosynthetic photon flux density (PPFD) of 500 µmol photons $m^{-2}$ $s^{-1}$. These plants were grown in plastic pots containing 2 kg of Andisol soil collected from Los Boldos-Lastarria (Araucanía Region, Chile) and maintained under these conditions for 2 weeks to allow acclimation. Subsequently, the plants were randomly assigned to two experimental groups. Group A consisted of control plants irrigated to maintain soil moisture at 80% of field capacity (FC). Group B comprised plants subjected to WD, which received irrigation at 50% FC. Soil moisture levels were monitored using capacitive sensors, and irrigation regimes were established according to protocols previously described by Bryla et al. [28] and Almutairi et al. [29].

### *2.2. Treatments*

After two weeks of acclimation, control plants were maintained under irrigation at 80% FC, whereas irrigation was withheld from the remaining plants until soil moisture reached 50% FC, corresponding to WD conditions as described previously by Almutairi et al. [29] and Chen et al. [30]. Soil moisture levels were monitored with calibrated sensors to ensure irrigation at 80% or 50% of field capacity (FC). The MeJA was applied by foliar spray at an effective dose of 50 µM MeJA previously determined by Cáceres et al. [17]. MeJA solution was prepared with 0.05% Tween 80 as the surfactant and applied in the early morning hours to maximize absorption efficiency, as described by Cáceres et al. [17,27]. The MeJA application volume was standardized at 25 mL per plant, based on the total foliar area required to achieve complete leaf coverage until runoff occurred. The solution was randomly sprayed throughout the aerial parts of the plants. To avoid drift of the MeJA solution between treatments, plants were separated using screens during application. For $Al^{3+}$ toxicity treatment, plants were treated with an Al chloride ($AlCl_3$) solution (18% $w/v$). A volume of 10 mL $AlCl_3$ per kilogram of soil was applied via irrigation to achieve an 70% Al saturation in soil as described by Slugeňová et al. [31] and Cáceres et al. [17,27]. Soil Al concentration and pH were maintained throughout the experiment and monitored at all sampling points (7, 14, and 21 days) through soil Al analysis. The experiment began once the Al was applied to the soil, and at the same time, the MeJA was sprayed once to the plants. A total of eight treatment groups with a pH of 4.5 ± 0.2 were established as follows: (i) Control: plants irrigated at field capacity without MeJA application; (ii) Positive control: control plants treated with MeJA; (iii) WD: plants irrigated at 50% field capacity; (iv) WD + MeJA: plants irrigated at 50% field capacity and treated with MeJA; (v) Al: plants subjected to 70% Al saturation; (vi) Al + MeJA: plants subjected to 70% Al saturation and treated with MeJA; (vii) Al + WD: plants subjected to 70% Al saturation and irrigated at 50% field capacity without MeJA and (viii) Al + WD + MeJA: plants subjected to combined Al stress and WD and treated with MeJA (Figure S1).

An additional group of five plants per treatment was allocated for growth measurements, which were performed at the end of the experiment. Sampling was conducted at 0, 7, 14, and 21 days (long-term) after the start of treatments. At each sampling time point, two highbush blueberry cultivars with contrasting Al resistance (Legacy as resistant and Star as sensitive) were collected. Each treatment consisted of five biological replicates (independent plants). For biochemical and enzymatic analyses, each biological replicate was measured in duplicate (technical replicates), and the mean value was used for statistical analyses. To

preserve sample integrity, plant tissues (leaves and roots) were rapidly immersed in liquid nitrogen immediately after collection and stored at −80 °C until further analyses.

### *2.3. Chemical Analyses of the Plants*

Dry shoot and root samples were ashed at 500 °C for 8 h. Subsequently, each sample was digested with 2 M HCl according to the method described by Sadzawka et al. [32]. Aluminum concentrations were determined using a simultaneous multielement atomic absorption spectrophotometer (Atomic Absorption Spectrometer, Model 969, Unicam, Cambridge, UK). This technique enabled accurate, precise quantification of Al concentration in plant samples.

### *2.4. Physiological Determinations*

#### 2.4.1. Plant Growth

Prior to the initiation of treatments, a subset of five plants was selected, and their shoots and roots were separated to determine fresh and dry weights (W1), which served as baseline measurements. The remaining plants were subjected to experimental treatments under the conditions described in Section 2.2. At the end of the experiment, five plants from each treatment were harvested, and shoot and root fresh and dry weights were determined (W2). Plant growth was quantified using the relative growth rate (RGR), calculated from the natural logarithm of mean plant weight using the following equation.

$$RGR = (\ln W2) - (\ln W1)/(t2 - t1),$$

where t1 represents the initial time (time 0) and t2 represents the final time (21 days) of the experiment [33].

#### 2.4.2. Total Auxins as Estimated by Salkowski-Reactive Indolic Compounds

Auxin extraction was performed using a solvent-induced phase transition extraction (SIPTE) described by Liu et al. [34], with 0.05, 0.1, and 0.15 g of plant material macerated with liquid nitrogen. Then, samples were incubated overnight in acetonitrile (0.5 mL for 0.05 g and 1 mL for 0.1–0.15 g of tissue). After phase separation, the lower fraction was dried in a concentrator for 2 h and resuspended in 1 mL of 30% (*v*/*v*) methanol. The total auxin concentration was quantified using the Salkowski colorimetric method [35], with modifications adapted for blueberry. Briefly, 200 µL of each sample was mixed with 50 µL of Salkowski's reagent, and the absorbance was measured at 530 nm in a Varioskan Flash microplate reader (Thermo Scientific, Wilmington, DE, USA). Indoleacetic acid (IAA) was used as the standard to generate the calibration curve.

#### 2.4.3. Plant Water Status

Leaf water potential (Ψw) and relative water content (RWC) were determined according to Begg and Turner [36] and Rahimi et al. [37], respectively. The Ψw of the shoot was measured in the morning (9 a.m.) using a Scholander chamber (Model 1000, PMS Instrument Co., Corvallis, OR, USA). Meanwhile, leaf RWC was determined using the following equation:

$$RWC = [(\text{fresh weight} - \text{dry weight})/(\text{turgor weight} - \text{dry weight})] \times 100.$$

#### 2.4.4. Net Photosynthesis (An) and Chlorophyll Fluorescence Parameters of PSII

$CO_2$ assimilation in intact, attached leaves was determined at 7, 14, and 21 days after the initiation of treatments using a portable infrared gas analyzer (IRGA) (LI-6400, LI-COR Inc., Lincoln, NE, USA) equipped with a chlorophyll fluorescence chamber. During

measurements, photosynthetically active radiation was set at 300 µmol $m^{-2}$ $s^{-1}$, and the reference $CO_2$ concentration was maintained at 400 ppm. In addition to net photosynthesis (An), transpiration rate (E), stomatal conductance (gs), photosynthetically active radiation (PAR), and leaf temperature were simultaneously recorded with the same instrument, as described by Ulloa-Inostroza et al. [16].

#### 2.4.5. Water-Use Efficiency (WUE) Determination

WUE was calculated as the ratio of the net photosynthetic rate (An) to the E. In addition, intrinsic WUE (WUEi) was calculated as An/gs [38].

#### 2.4.6. Chlorophyll Fluorescence Parameters

The maximum quantum efficiency of photosystem II (Fv/Fm), effective quantum yield of PSII (ΦPSII), photochemical quenching (qP), non-photochemical quenching (qN), and electron transport rate (ETR) were assessed at 7, 14, and 21 days after treatment initiation. Measurements were conducted using a portable infrared gas exchange analyzer (IRGA; LI-6400, LI-COR Inc., Lincoln, NE, USA), following the methodology reported by Reyes-Díaz et al. [13].

### *2.5. Biochemical Analysis*

#### 2.5.1. Photosynthetic Pigments

Photosynthetic pigments were extracted using 100% HPLC-grade acetone, with samples maintained at 4 °C and handled under dim green light to minimize photooxidative degradation. Extracts were subsequently centrifuged at 4 °C to remove insoluble material. Chlorophyll a, chlorophyll b, and the carotenoids violaxanthin, antheraxanthin, zeaxanthin, and lutein were quantitatively determined as indicators of photosynthetic performance and photoprotective capacity. Pigment analysis was performed by high-performance liquid chromatography coupled with a diode-array detector (HPLC-DAD, JASCO, LCNet II/ADC, Tokyo, Japan), following the method described by García-Plazaola and Becerril [39].

#### 2.5.2. Lipid Peroxidation

Lipid peroxidation was determined as an indicator of oxidative damage using the thiobarbituric acid reactive substances (TBARS) assay [40]. Fresh leaf and root tissues (200 mg) were weighed and homogenized in 2 mL of 0.1% (*w*/*v*) trichloroacetic acid (TCA) buffer using a chilled mortar and pestle on ice. Homogenization was performed for 5 min, followed by centrifugation at 12,000 rpm for 15 min at 4 °C. An aliquot of 1 mL of the supernatant was mixed with 4 mL of 0.5% (*w*/*v*) thiobarbituric acid (TBA) prepared in 20% TCA. The reaction mixtures were incubated in a water bath at 95 °C for 30 min, then rapidly cooled on ice to stop the reaction. Absorbance was measured at 532 nm, corresponding to the maximum absorbance of malondialdehyde (MDA), and at 600 nm to correct for nonspecific turbidity, using a UV/Vis spectrophotometer (UNICOR SpectroQuest 2800, UV/VIS, Barcelona, Spain). MDA concentration was calculated using a molar extinction coefficient of 155 $mM^{-1}$ $cm^{-1}$ and expressed as nmol MDA $g^{-1}$ fresh weight.

#### 2.5.3. Total Soluble Phenols

Total soluble phenols were quantified using the Folin–Ciocalteu reagent, following the method of Singleton and Rossi [41], with modifications for blueberry samples. Fresh leaves/root tissues (200 mg) were weighed, and phenolic compounds were extracted with 2 mL of 80% (*v*/*v*) ethanol in Falcon tubes. The absorbance was measured at 765 nm using a UV/Vis spectrophotometer (UNICOR SpectroQuest 2800, UV/VIS, Spain). Results were expressed as chlorogenic acid equivalents (CAE) and reported as mg $g^{-1}$ fresh weight.

2.5.4. Free Radical Scavenging Activity (AA)

The antioxidant activity (AA) was determined using the 2,2-diphenyl-1-picrylhydrazyl (DPPH) free radical scavenging assay, based on the reduction in the DPPH radical by antioxidants present in the plant extracts. The absorbance was measured at 515 nm using a spectrophotometer (UNICOR Spectro Quest 2800, UV/VIS, Spain) with Trolox as the standard. The values were expressed in μg Trolox equivalents g−1 fresh weight (FW) [42].

2.5.5. Determination of Enzyme Superoxide Dismutase (SOD)

Fresh plant tissue (10 mg) was weighed and homogenized in 1.5 mL of enzyme-specific extraction buffer. The homogenates were centrifuged at 12,000 rpm for 20 min at 4 °C. The supernatants were collected and used for subsequent enzymatic assays. SOD activity was determined by photochemical reduction in nitroblue tetrazolium (NBT). The reaction mixture was prepared with 119 μL of phosphate buffer (50 mM, pH 7.8), 10 μL of methionine (13 mM), 15 μL of NBT (75 μM), 2 μL of EDTA (0.1 mM), and 34 μL of riboflavin (2 μM). The reaction was initiated by adding 20 μL of enzyme extract and incubating the mixture under fluorescent light for 15 min. The absorbance was measured at 560 nm, and SOD activity was expressed as enzymatic units per milligram of protein (U $mg^{-1}$ protein), defined as the amount of enzyme required to cause 50% inhibition of NBT reduction [43]. The protein concentration was determined by the Bradford method [44]. Aliquots of 200 μL of enzyme extract were used, and absorbance was measured at 595 nm. Protein concentration was calculated by comparison with a standard curve generated using bovine serum albumin (BSA).

### *2.6. Statistical Analysis*

The experiment was conducted using a completely randomized design with a three-way factorial arrangement, with cultivar, treatment, and exposure time as fixed factors. For the analysis, five biological replicates and two technical replicates were considered for each cultivar, treatment, and time. To ensure the validity of the statistical analysis, all data were tested for normality and homogeneity of variance using the Kolmogorov–Smirnov test. If these assumptions were met, data were subjected to analysis of variance (ANOVA), and mean comparisons were performed using Tukey's post hoc test. All statistical analyses were carried out using SigmaStat software version 3.0 (SigmaStat, San José, CA, USA). Correlation analyses were performed to evaluate relationships between independent variables, particularly internal Al concentration, and selected dependent variables obtained from physiological and biochemical measurements. In addition, multivariate analyses, including principal component analysis (PCA), multiple correlation analysis, and heatmap visualization, were conducted using the RStudio 2026.05.0+218 version statistical environment.

## 3. Results

### *3.1. Aluminum Accumulation and Growth-Related Hormonal Response in Blueberries Under Combined WD-Al Stress*

Aluminum (Al) concentrations in *V. corymbosum* L. (Legacy and Star cultivars) showed statistically significant differences across treatments, cultivars, exposure time, and, mainly, their interactions ($p < 0.001$) (Figure 1A,B). Al values ranged from 80 to 550 mg/kg in the leaves (Figure 1A) and from 1200 to 6000 mg/kg in roots (Figure 1B). This distribution represents a characteristic pattern of $Al^{3+}$ toxicity, with preferential accumulation in roots. Compared with the control, Al treatment significantly increased Al concentration in both leaves (200–350%) and roots (up to 600–700%). In contrast, WD alone did not affect tissue Al levels in both cultivars, remaining close to the reference values. Under combined stress

(Al + WD), Al concentration was reduced by 25–40% compared with Al treatment alone in both organs (Figure 1A,B). This suggests that the water limitation partially restricted the uptake or translocation of Al. Nevertheless, plants subjected to Al + WD maintained higher tissue Al concentrations than those under WD alone.

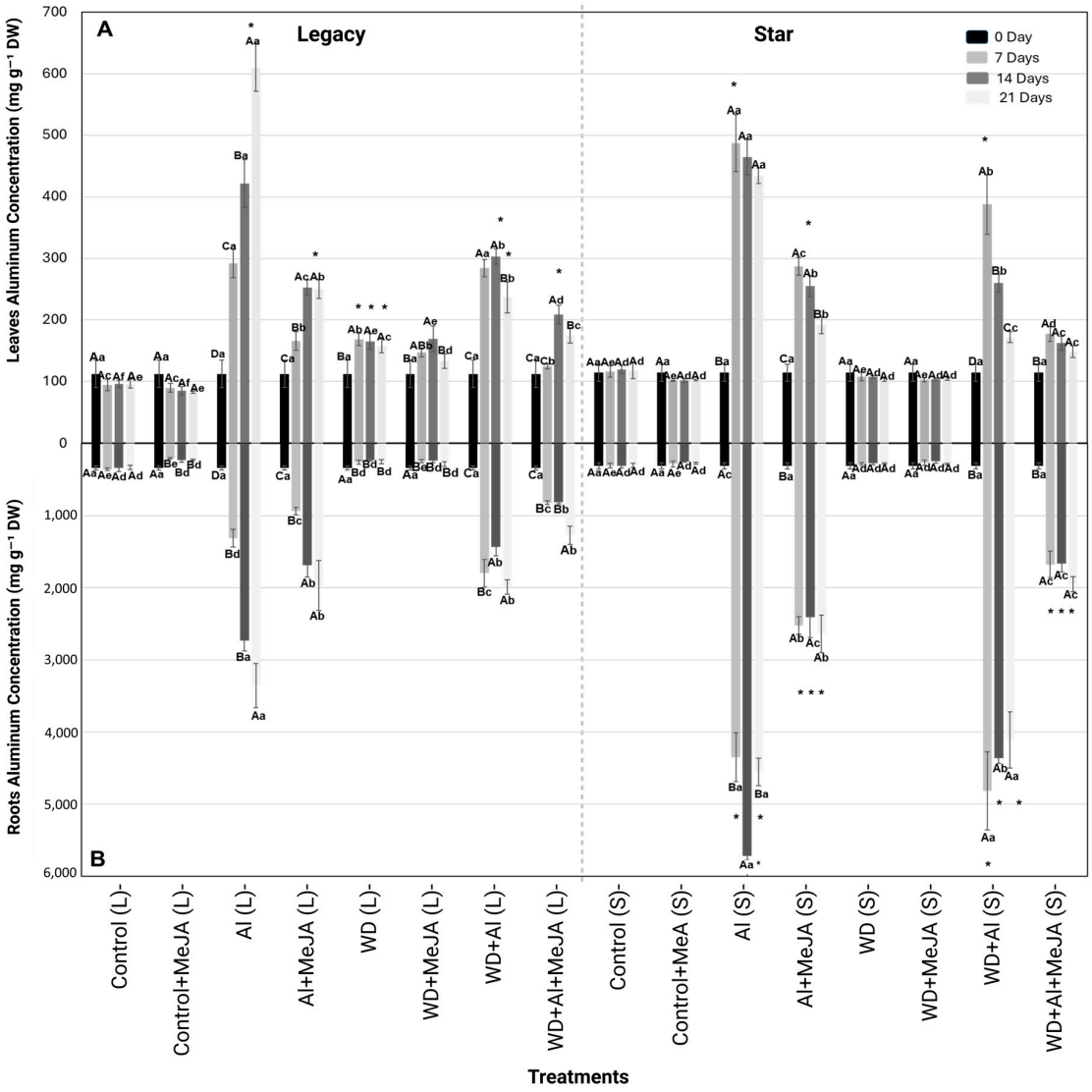


**Figure 1.** Aluminum concentration in tissues of *V. corymbosum* L. cultivars Legacy and Star, under combined stress (Al + WD) and application of MeJA. (**A**) Leaves. (**B**) Roots. Treatments included: Control, Aluminum (Al), WD, and combinations with MeJA (Control + MeJA, Al + MeJA, WD + MeJA, Al + WD + MeJA). Different capital letters indicate significant differences among times within each cultivar and treatment (ANOVA, Tukey HSD, $p < 0.05$). Different lower case letter indicate significant differences among treatments with each cultivar and time (ANOVA, Tukey HSD, $p < 0.05$). Asterisks (*) indicate significant differences between cultivars for the same treatment and time.

The presence of MeJA significantly reduced Al accumulation in leaves and roots (Figure 1A,B). Under Al + MeJA, Al levels decreased by an average of 35–45% compared to Al, whereas in Al + WD + MeJA the reduction reached 30–35% compared to Al + WD. In contrast, MeJA application under non-stress conditions (Control + MeJA) or under WD alone (WD + MeJA) did not alter Al concentrations, which remained similar to their respective controls, suggesting that MeJA primarily modulates plant responses under Al stress conditions. Between the cultivars, Star consistently accumulated 20–35% more Al than Legacy, with the difference most pronounced in the roots at 21 days. Legacy showed

a more effective response to MeJA application, as indicated by a reduction in tissue Al concentration in both leaves and roots (Figure 1A,B). Overall, the results show that Al accumulates preferentially in the roots, with lower levels under combined stress than under Al alone (Figure 1B). Exogenous MeJA application effectively mitigated metal uptake and translocation, with a more favorable response in Legacy, demonstrating its protective role against Al toxicity.

The relative growth rate (RGR) of *V. corymbosum* L. (Legacy and Star cultivars), expressed on a dry weight (DW) basis, showed very significant differences depending on the treatment, cultivar, and interaction between factors ($p < 0.001$) (Figure 2A,B). The values ranged from 0.04 to 0.18 g DW day$^{-1}$ in the leaves and from 0.01 to 0.07 g DW day$^{-1}$ in the roots. The reduction in growth was most pronounced in Star at 21 days, in both leaves and roots. In general, roots showed a stronger decline in RGR than leaves across treatments (Figure 2A,B), consistent with the Al concentration analysis above (Figure 1A,B).

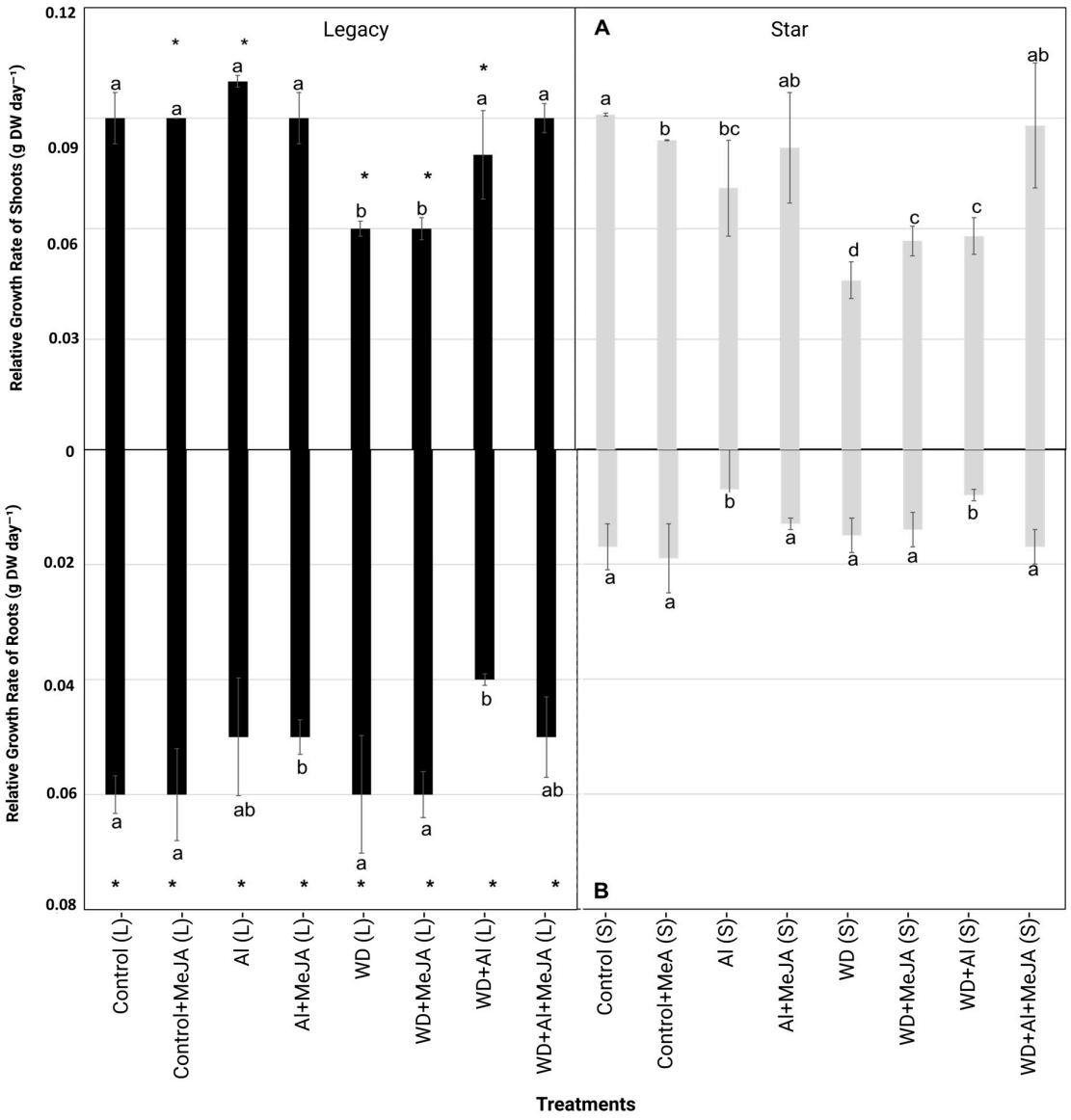


**Figure 2.** Relative Growth Rate (RGR) in the tissues of *V. corymbosum* L. cultivars Legacy and Star, under combined stress (Al + WD) and application of MeJA at 21 days. (**A**) Shoots. (**B**) Roots. Treatments: Control + MeJA, Al + MeJA, WD + MeJA, Al + WD + MeJA. Different lower case letters indicate significant differences among treatments within each cultivar (ANOVA, Tukey HSD, $p < 0.05$). Asterisks (*) indicate significant differences between cultivars for the same treatment.

WD caused the greatest reduction in RGR in both tissues, with average decreases of 30–40% in leaves and up to 50% in roots compared to the control. The Al treatment induced moderate reductions of 15–25% in leaves and 20–35% in roots. Combined stress (Al + WD) showed the lowest growth rates, with decreases of 35–50% in leaves and up to 60% in roots compared with the control. The MeJA application partially mitigated these effects. Under Al + MeJA, the RGR increased by 15–25% compared to Al alone, while in WD + MeJA, it showed a 20–30% improvement compared to WD, mainly in Legacy, with this effect being more noticeable in the roots (Figure 1B). Under combined stress (Al + WD + MeJA), RGR increased by 15–25% compared to Al + WD. However, values remained below those of the control. Legacy consistently maintained higher RGR values than Star, exceeding it by up to 20% in leaves and 30% in roots. Following MeJA application under stress conditions, Legacy recovered RGR to approximately 80% of control values at 21 days, whereas Star recovered to only about 60%. These results indicate that the combined stress (Al + WD) was the most limiting condition for growth, particularly in roots. That exogenous MeJA partially mitigated growth inhibition, with a stronger effect observed in Legacy.

Total auxin concentrations as estimated by Salkowski-reactive indolic compounds in leaves and roots of *V. corymbosum* L. (Legacy and Star cultivars) showed highly significant effects of treatment, time, and interaction among factors ($p < 0.001$) (Figure 3A,B). Total auxin concentrations ranged from 900 to 3100 µg IAA eq·g$^{-1}$ FW in the leaves (Figure 3A) and from 100 to 600 µg IAA eq·g$^{-1}$ FW in roots (Figure 3B), indicating substantially higher auxin levels in leaves than in roots. In both tissues, auxin concentrations declined markedly under stress conditions, especially under WD, with reductions of 35–45% in leaves and 50–55% in roots relative to the control. Combined stress (Al + WD) resulted in the greatest reduction in auxin concentration, reaching 45–50% in leaves and up to 60% in roots relative to the control. Al treatment alone reduced auxin levels by approximately 30%, with a more pronounced effect in Star.

The application of MeJA partially mitigated stress-induced reductions in auxin concentration, resulting in significant increases in both tissues, including under non-stress conditions (Control + MeJA). Under Al + MeJA treatments, auxin levels increased by 20–25% compared to Al alone, while in WD + MeJA increased by 25–35% compared to WD. In the combined treatment (Al + WD + MeJA), auxin concentration recovered by 30–40% in leaves and 50–55% in roots relative to Al + WD. These results support a modulatory effect of MeJA on auxin concentrations under stress conditions.

Under non-stress conditions, MeJA-treated plants (Control + MeJA) exhibited auxin concentrations similar to or slightly higher (5–40%) than those observed in untreated control plants, indicating a stimulatory effect on basal auxin levels. Across treatments, Legacy consistently showed higher auxin concentrations than Star, with differences of 15–25% in leaves and 20–30% in roots (Figure 3A,B). The effect of MeJA under stress conditions was more pronounced in Legacy, in which auxin concentrations were maintained close to control levels even under combined stress (Al + WD). In contrast, Star showed only partial recovery, reaching approximately 60% of its respective control values. In Star, the largest reductions in auxin concentration were consistently observed across all stress treatments, suggesting heightened hormonal regulation sensitivity under stress. Overall, auxin concentrations were significantly reduced by both Al and WD, with stronger effects observed in roots than in leaves. This correlated with reductions in RGR and Al accumulation patterns. Combined stress (Al + WD) resulted in the most significant decline in auxin levels. The application of exogenous MeJA partially restored auxin concentrations, particularly in the Legacy variety, suggesting an association between jasmonate treatment and the maintenance of auxin concentration under abiotic stress conditions.

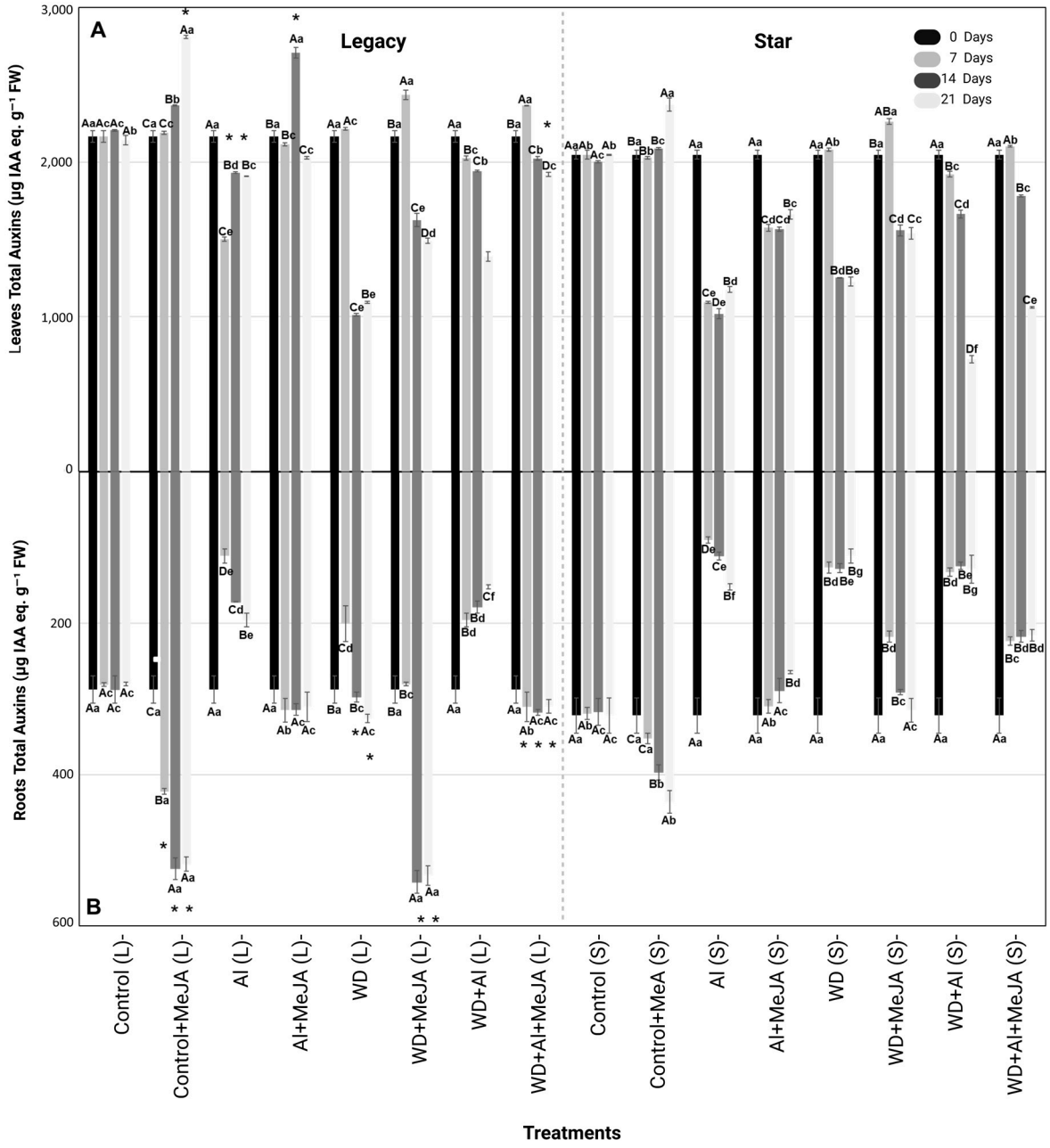


**Figure 3.** Total auxins measured by Salkowski method in the tissues of *V. corymbosum* L. cultivars Legacy and Star, under combined stress (Al + DW) and application of MeJA. (**A**) Leaves, and (**B**) Roots. Treatments included: Control, Aluminum (Al), WD, and combinations with MeJA (Control + MeJA, Al + MeJA, WD + MeJA, Al + WD + MeJA). Different capital letters indicate significant differences among times within each cultivar and treatment (ANOVA, Tukey HSD, $p < 0.05$). Different lower case letter indicate significant differences among treatments with each cultivar and time (ANOVA, Tukey HSD, $p < 0.05$). Asterisks (*) indicate significant differences between cultivars for the same treatment and time.

### *3.2. Water Status and Osmotic Adjustment in Vaccinium corymbosum L. Under Aluminum Stress and Water Deficit*

The water status determined at the leaf level for *V. corymbosum* L. (Legacy and Star cultivars) showed significant differences depending on the treatment, cultivar, exposure time, and interaction among factors for leaf water potential (Ψw, $p < 0.001$) and relative water content (RWC, $p < 0.05$) (Figure 4A,B). The leaf water potential (Ψw) values obtained in the morning (9 a.m.) ranged from −0.5 to −2.9 MPa, showing a very marked decrease

at 21 days. In general, the decrease in water potential was more pronounced under WD and combined stress (Al + WD) (Figure 4B). Compared with the control (−0.5 MPa), the Al treatment reduced water potential to values of approximately 80–100%. WD intensified the decrease, resulting in reductions of 140–170%. The most negative values were observed under combined stress (Al + WD), reaching −2.6 to −2.9 MPa, particularly in the Star cultivar (Figure 4B).

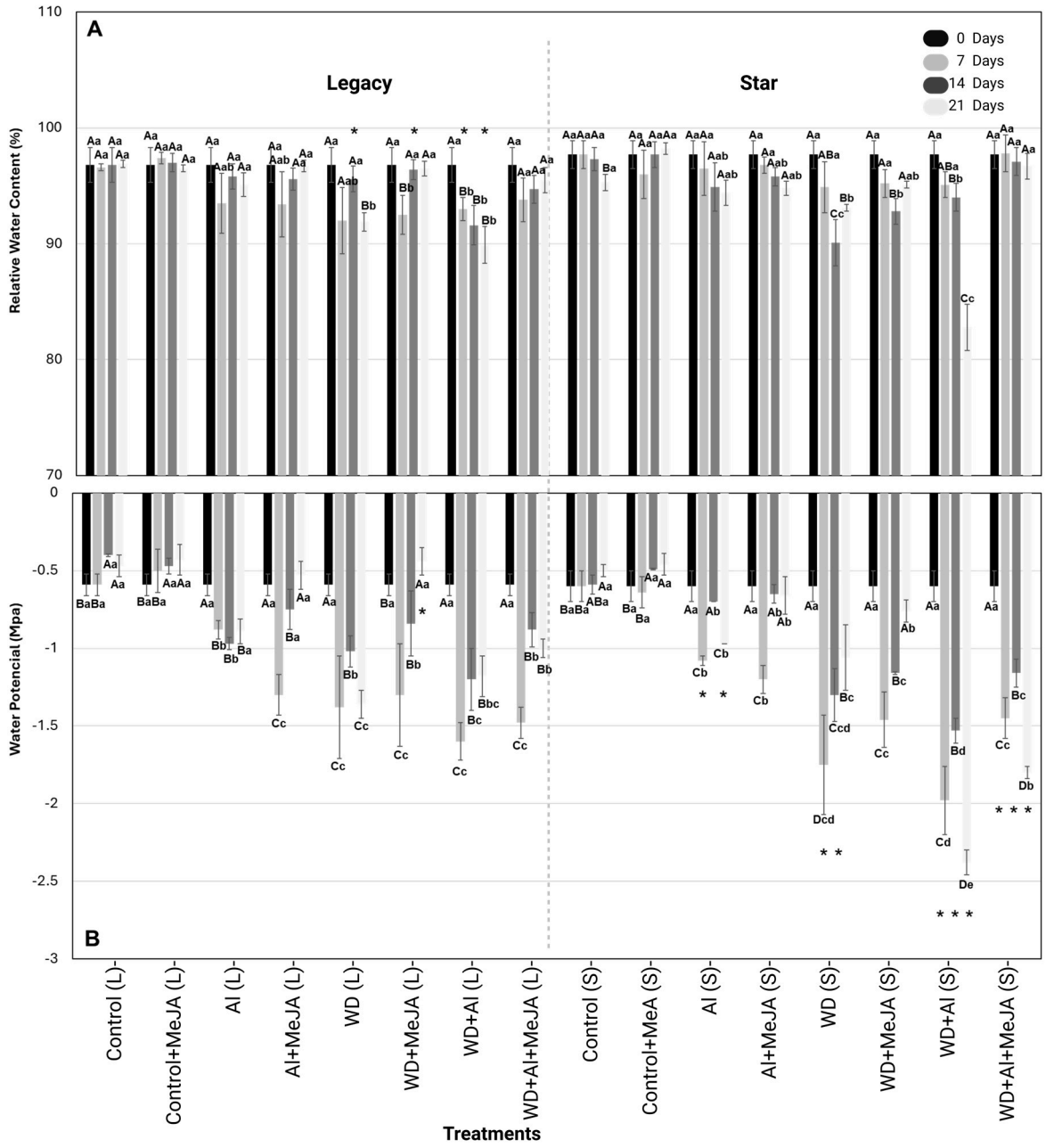


**Figure 4.** Water status of *V. corymbosum* L. cultivars Legacy and Star, under combined stress (Al + WD) and application of MeJA. (**A**) Relative Water Content. (**B**) Water potential (Mpa). Treatments included: Control, Aluminum (Al), WD, and combinations with MeJA (Control + MeJA, Al + MeJA, WD + MeJA, Al + WD + MeJA). Different capital letters indicate significant differences among times within each cultivar and treatment (ANOVA, Tukey HSD, $p < 0.05$). Different lower case letter indicate significant differences among treatments with each cultivar and time (ANOVA, Tukey HSD, $p < 0.05$). Asterisks (*) indicate significant differences between cultivars for the same treatment and time.

Exogenous application of MeJA partially mitigated the decline in leaf water potential across all stress treatments. For Al + MeJA, Ψw improved by 15–25% compared to Al, whereas WD + MeJA showed an approximately 20% improvement relative to WD. Under combined stress, Al + WD + MeJA increased Ψw by up to 30% compared with Al + WD. When comparing cultivars, Star consistently showed more negative Ψw values than Legacy, with differences of 0.1–0.3 MPa, across most treatments and lowest values under WD and Al + WD, indicating greater susceptibility to water loss in Star. In contrast, Legacy maintained more stable Ψw values and showed a stronger recovery following MeJA application, reaching 80–85% of control levels, whereas Star recovered only 60–65% (Figure 4B).

The relative water content (RWC) in *V. corymbosum* L. leaves ranged from 70 to 98%, with a progressive decline over time; the greatest reductions were observed at 21 days (Figure 4A). Compared with control (97%), treatment with Al reduced leaf RWC by 5–8%. WD caused more marked decreases, reaching reductions of 8–12%, whereas combined stress (Al + WD) was the most severe, with RWC reductions of 12–15% relative to the control (Figure 4A). This pattern was consistent with the decline in leaf water potential observed under stress conditions (Figure 4B). Exogenous MeJA partially alleviated the reductions in RWC under all stress treatments. In Al + MeJA, RWC increased by 4–6% compared with Al, whereas WD + MeJA and Al + WD + MeJA showed recoveries of 6–9% relative to their respective stress treatments (Figure 4A). Among cultivars, Legacy consistently maintained slightly higher RWC values than Star, with the largest differences observed under combined stress. Overall, WD and Al + WD produced the strongest reductions in leaf water status, particularly at 21 days, while MeJA application mitigated water loss and favored the maintenance of leaf hydration, especially in Legacy.

Proline concentration was determined in leaves and roots of *V. corymbosum* L. (Legacy and Star cultivars) to assess osmotic adjustment. Significant differences were observed among treatments, cultivars, sampling times, and their interactions ($p < 0.001$) (Figure 5A,B). Proline levels ranged from 4 to 13 μmol $g^{-1}$ FW in leaves (Figure 5A) and from 10 to 45 μmol $g^{-1}$ FW in roots (Figure 5B), with higher accumulation in the root system and at 7 days of treatment. Compared to the control, the Al treatment increased foliar proline concentration by approximately 60–70%, reaching values close to 9 μmol $g^{-1}$ FW, whereas WD caused more pronounced increases of 90–100% compared to the control (10–11 μmol $g^{-1}$ FW). Combined stress (Al + WD) generated the highest accumulation, with increases of 130–150%. In roots, the pattern was similar but with higher relative values: Al increased the concentration by 60–80%, WD by 130–150%, and Al + WD by 200–230% compared to the control, reaching up to 45 μmol $g^{-1}$ FW (Figure 5B). These results reflect a marked initial osmotic response to dehydration and metal toxicity, with the effect of WD and combined stress predominating, although this decreases over time.

Exogenous MeJA significantly modulated proline accumulation in both tissues, reducing the stress-induced increase while maintaining levels above the control. Proline concentrations decreased by approximately 15–25% in leaves and 20–30% in roots compared with the respective stress treatments without MeJA (Figure 5). Differences between cultivars were also evident, with Star accumulating higher proline levels than Legacy, particularly during the early stages under WD and Al + WD. Overall, proline accumulation was strongest under WD and combined stress, whereas MeJA partially reduced this response. Legacy showed a more controlled adjustment, while Star exhibited greater proline accumulation under severe stress conditions.

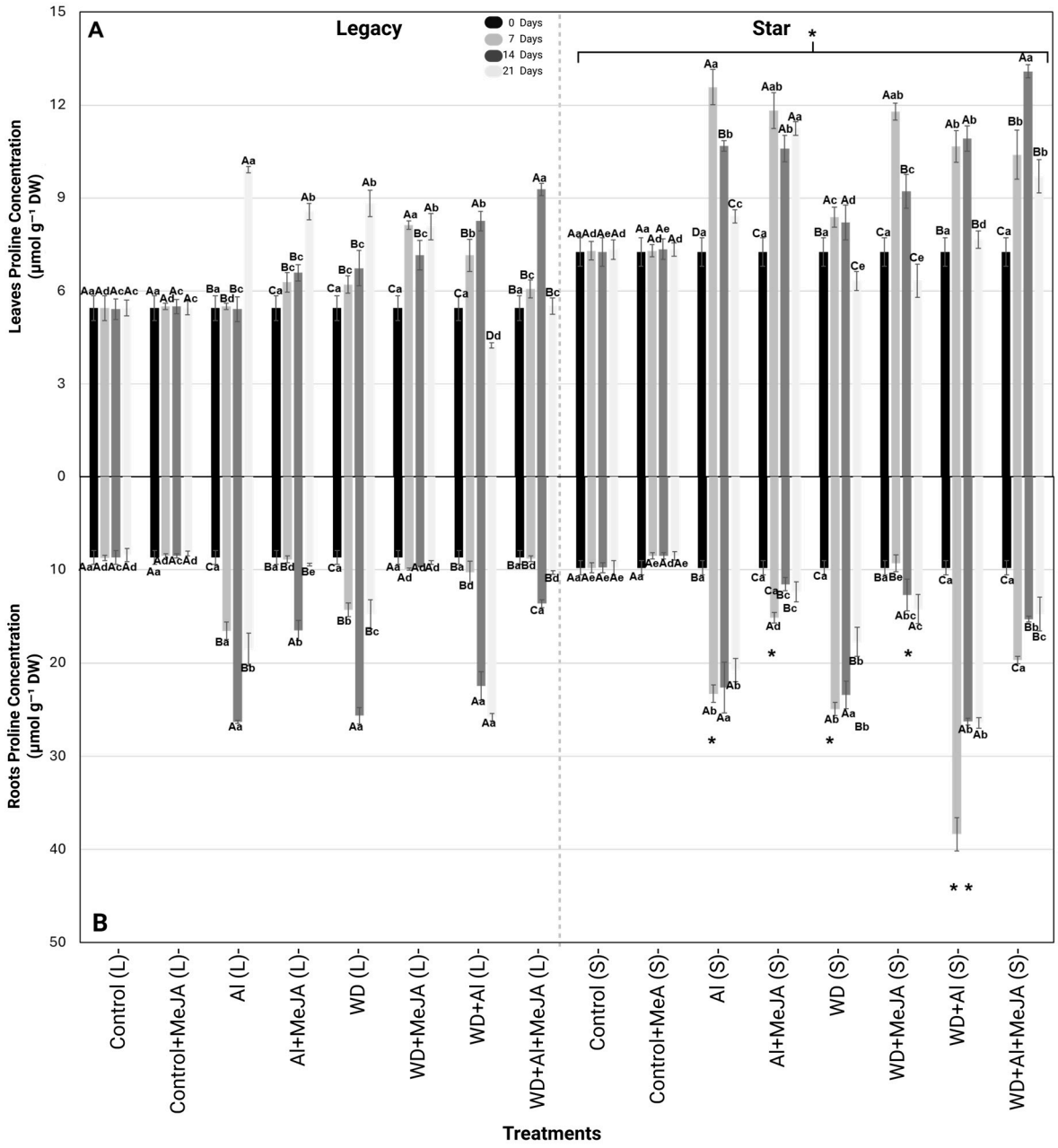


**Figure 5.** Proline concentration of *V. corymbosum* L. cultivars Legacy and Star, under combined stress (Al + WD) and application of MeJA. (**A**) Leaves, and (**B**) Roots. Treatments included: Control, Aluminum (Al), WD, and combinations with MeJA (Control + MeJA, Al + MeJA, WD + MeJA, Al + WD + MeJA). Different capital letters indicate significant differences among times within each cultivar and treatment (ANOVA, Tukey HSD, $p < 0.05$). Different lower case letter indicate significant differences among treatments with each cultivar and time (ANOVA, Tukey HSD, $p < 0.05$). Asterisks (*) indicate significant differences between cultivars for the same treatment and time.

### *3.3. Photosynthetic Performance and Water Use Efficiency in Vaccinium corymbosum L. Under Aluminum Stress and Water Deficit*

Photosynthetic performance in *V. corymbosum* leaves was evaluated using gas exchange parameters, including An, gs, and E, together with water use efficiency, both intrinsic (WUEi = An/gs) and apparent (WUE = An/E), as well as chlorophyll fluorescence parameters of photosystem II (Fv/Fm, ΦPSII, qP, qN, and ETR). All variables showed significant differences among treatments, sampling times, and their interactions ($p < 0.001$) (Figure 6, Tables 1 and 2). No clear temporal trends were observed. However, both cultivars

showed a consistent response pattern, with WD and combined stress (Al + WD) producing the strongest reductions in photosynthetic performance and water use efficiency.

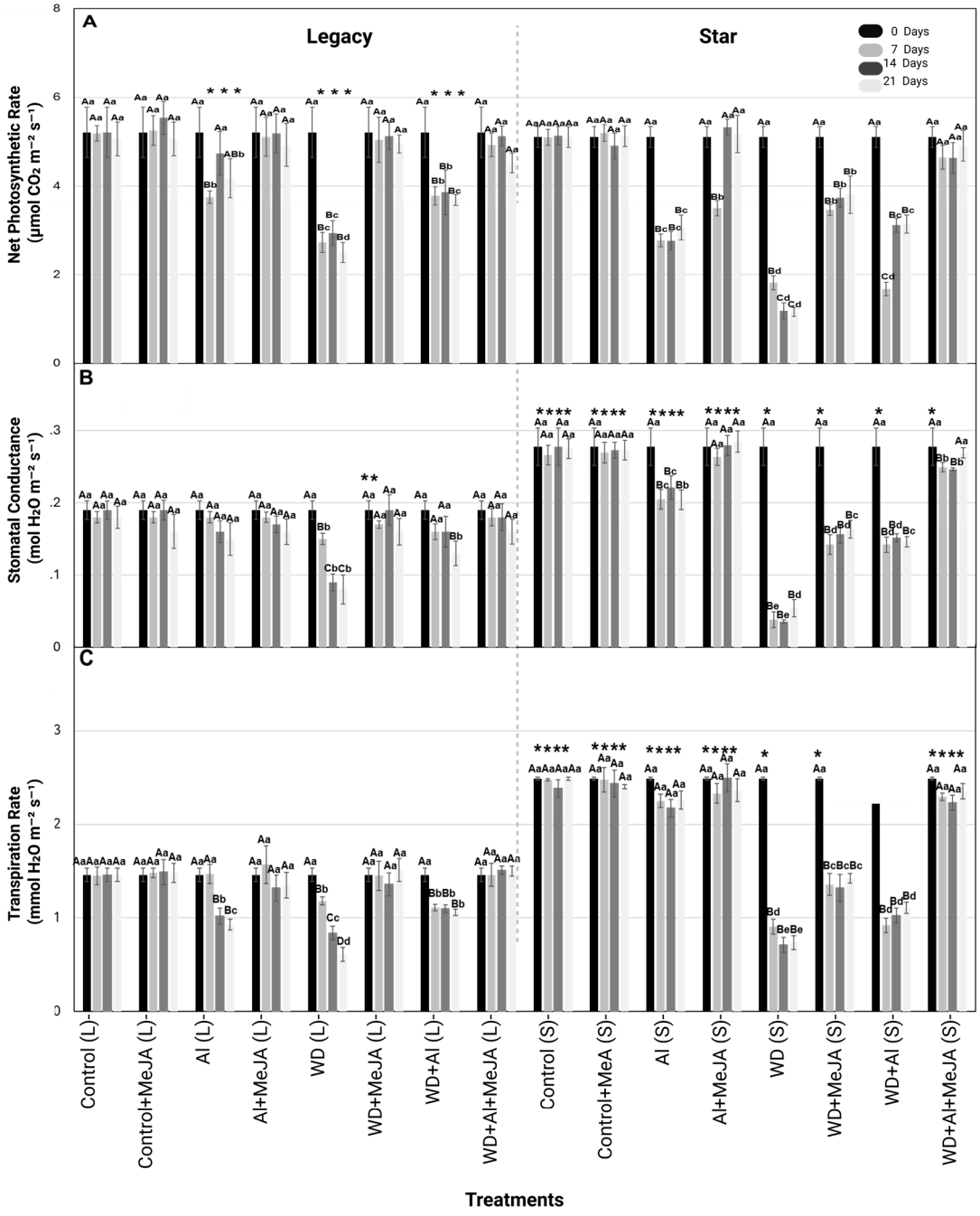


**Figure 6.** Photosynthetic parameters of *V. corymbosum* L. cultivars Legacy and Star, under combined stress (Al + WD) and application of MeJA. (**A**) Photosynthesis net (An). (**B**) Stomatal Conductance (gs). (**C**) Transpiration. Treatments included: Control, Aluminum (Al), WD, and combinations with MeJA (Control + MeJA, Al + MeJA, WD + MeJA, Al + WD + MeJA). Different capital letters indicate significant differences among times within each cultivar and treatment (ANOVA, Tukey HSD, $p < 0.05$). Different lower case letter indicate significant differences among treatments with each cultivar and time (ANOVA, Tukey HSD, $p < 0.05$). Asterisks (*) indicate significant differences between cultivars for the same treatment and time.

Net photosynthesis ranged from 2.0 to 6.0 µmol $CO_2$ $m^{-2}$ $s^{-1}$ (Figure 6A). WD produced the strongest limitation to $CO_2$ assimilation, reducing An by 45–60% relative to the

control. Combined stress (Al + WD) also markedly decreased photosynthesis (35–50%), whereas Al alone caused more moderate reductions of up to 30%. Exogenous MeJA promoted an almost total recovery of photosynthetic performance (Figure 6A). An increase of 25–40% in Al + MeJA and by 40–60% in WD + MeJA relative to their respective stress treatments, with both reaching control values (Figure 6A). Under combined stress, MeJA also promoted partial recovery, with An increase of 30–45% compared with Al + WD. The Control + MeJA treatment showed a slight stimulation of photosynthesis (up to 10%), suggesting a basal-promoting effect of jasmonate. Across treatments, Legacy maintained consistently higher An values than Star (ca. 20%). Moreover, MeJA-induced recovery was more stable in Legacy, which often returned to control levels (Figure 6A).

**Table 1.** Water use efficiency of *V. corymbosum* L. cultivars Legacy and Star, under conditions of combined stress (Al + WD) and application of MeJA. Treatments included: Control, Aluminum (Al), WD, and combinations with MeJA (Control + MeJA, Al + MeJA, WD + MeJA, Al + WD + MeJA). Different capital letters indicate significant differences among treatments within each cultivar and time (ANOVA, Tukey HSD, $p < 0.05$). Different lower case letter indicate significant differences among treatments with each cultivar and time (ANOVA, Tukey HSD, $p < 0.05$). Asterisks (*) indicate significant differences between cultivars for the same treatment and time.

| | | WUEi (An/gs) | | WUE (An/E) | |
|---|---|---|---|---|---|
| **Time** | **Treatments** | **Legacy** | **Star** | **Legacy** | **Star** |
| 7D | Control | 28.6 Aa * | 19.2 Abc | 3.6 Aa * | 2.1 Ab |
| | Control + MeJA | 29.4 Aa * | 19.3 Abc | 3.6 Aa * | 2.1 AB |
| | Al | 20.5 Bb * | 13.6 Ac | 2.5 Ab * | 1.2 Ab |
| | Al + MeJA | 28.7 Aa * | 13.3 c | 3.3 Aab * | 1.5 Ac |
| | WD | 18.1 Bb * | 47.7 Aa * | 2.3 Ab * | 2.0 Ab |
| | WD + MeJA | 29.2 Aa | 24.3 Ab | 3.5 Aa * | 2.6 Aa |
| | Al + WD | 23.9 Bab * | 11.8 Bc | 3.4 Aab * | 1.8 Ab |
| | Al + WD + MeJA | 27.7 Aa * | 18.6 Abc | 3.4 Aab * | 2.0 Ab |
| 14D | Control | 27.7 Aa * | 18.5 Ac | 3.6 Ac * | 2.2 Ab |
| | Control + MeJA | 28.8 Aa * | 18.0 Ac | 3.7 Ab * | 2.0 Ab |
| | Al | 29.9 Aa * | 12.5 Ad | 4.7 Ba * | 1.3 Ad |
| | Al + MeJA | 30.3 Aa * | 19.1 Ac | 3.9 Bb * | 2.1 Bb |
| | WD | 31.9 Aa | 33.3 Ba | 3.5 Bc * | 1.7 Ac |
| | WD + MeJA | 26.9 Aa | 23.8 Ab | 3.8 Ab * | 2.8 Aa |
| | Al + WD | 24.8 Bb | 20.5 Ac | 3.5 Ac * | 3.0 Aa |
| | Al + WD + MeJA | 29.1 Aa * | 18.8 Ac | 3.4 Ac * | 2.1 Bb |
| 21D | Control | 28.4 Aa * | 18.6 Ab | 3.5 Ac * | 2.1 Ab |
| | Control + MeJA | 30.9 Aa * | 18.8 Ab | 3.4 Ac * | 2.1 Ab |
| | Al | 27.6 Aa * | 15.0 Ac | 4.5 Aa * | 1.4 Ac |
| | Al + MeJA | 30.1 Aa * | 18.2 Ab | 3.7 Ac * | 2.2 Ab |
| | WD | 30.6 Aa * | 21.3 Ca * | 4.1 Ab * | 1.6 Ac |
| | WD + MeJA | 30.2 Aab * | 23.3 Aa | 3.3 Acd * | 2.7 Aa |
| | Al + WD | 29.0 Ab | 21.5 Ab | 3.5 Ac * | 2.8 Aa |
| | Al + WD + MeJA | 28.0 Aab * | 18.2 Ab | 3.0 Ad * | 2.1 Ab |

**Table 2.** Fluorescence parameters of *V. corymbosum* L. cvs. Legacy and Star, under conditions of combined stress (Al + WD) and application of MeJA. Treatments included: Control, Aluminum (Al), WD, and combinations with MeJA (Control + MeJA, Al + MeJA, WD + MeJA, Al + WD + MeJA). Different lower case letter indicate significant differences among treatments with each cultivar and time (ANOVA, Tukey HSD, $p < 0.05$).

| | | Fv/Fm | | ΦPSII | | qP | | qN | | ETR | |
|---|---|---|---|---|---|---|---|---|---|---|---|
| **Time** | **Treatments** | **Legacy** | **Star** | **Legacy** | **Star** | **Legacy** | **Star** | **Legacy** | **Star** | **Legacy** | **Star** |
| 7D | Control | 0.80 b | 0.80 a | 0.184 b | 0.166 c | 0.252 ab | 0.176 a | 0.748 g | 0.824 i | 40.1 b | 38.2 a |
| | Control + MeJA | 0.80 b | 0.82 b | 0.187 b | 0.169 c | 0.263 a | 0.171 ab | 0.744 g | 0.824 i | 40.6 b | 38.8 a |
| | Al | 0.80 b | 0.76 g | 0.123 e | 0.075 g | 0.135 g | 0.115 g | 0.845 c | 0.885 d | 26.7 e | 16.3 g |
| | Al + MeJA | 0.81 a | 0.79 c | 0.149 d | 0.153 d | 0.173 e | 0.167 b | 0.794 e | 0.833 g | 32.4 cd | 33.3 c |
| | WD | 0.79 d | 0.74 e | 0.084 | 0.058 i | 0.138 g | 0.082 j | 0.862 b | 0.918 a | 18.2 h | 12.7 h |
| | WD + MeJA | 0.80 b | 0.78 i | 0.201 a | 0.119 f | 0.253 b | 0.174 a | 0.747 g | 0.826 h | 43.6 a | 25.9 e |
| | Al + WD | 0.79 c | 0.74 i | 0.094 g | 0.062 i | 0.158 f | 0.099 i | 0.842 c | 0.901 b | 20.5 g | 13.5 h |
| | Al + WD + MeJA | 0.79 d | 0.79 d | 0.140 e | 0.131 e | 0.238 c | 0.146 e | 0.762 f | 0.819 j | 30.5 d | 28.5 d |
| 14D | Control | 0.81 a | 0.80 b | 0.181 b | 0.177 b | 0.251 ab | 0.174 a | 0.749 g | 0.826 h | 39.3 b | 38.5 b |
| | Control + MeJA | 0.80 b | 0.81 a | 0.182 b | 0.174 b | 0.258 a | 0.176 a | 0.742 g | 0.824 i | 39.6 b | 38.8 b |
| | Al | 0.78 e | 0.76 f | 0.105 f | 0.099 h | 0.136 g | 0.176 a | 0.864 b | 0.824 i | 22.9 f | 21.5 f |
| | Al + MeJA | 0.80 b | 0.79 c | 0.155 d | 0.173 b | 0.180 d | 0.173 ab | 0.820 d | 0.827 h | 34.8 c | 37.6 b |
| | WD | 0.77 f | 0.75 hi | 0.077 i | 0.070 g | 0.141 g | 0.108 h | 0.859 b | 0.892 c | 16.8 i | 15.2 g |
| | WD + MeJA | 0.79 c | 0.79 c | 0.186 b | 0.133 e | 0.239 c | 0.176 a | 0.761 g | 0.824 i | 40.4 b | 28.9 d |
| | Al + WD | 0.77 f | 0.75 h | 0.078 i | 0.116 f | 0.137 g | 0.156 d | 0.863 b | 0.844 f | 16.9 i | 25.2 e |
| | Al + WD + MeJA | 0.79 bc | 0.79 cd | 0.171 c | 0.183 b | 0.254 b | 0.156 d | 0.746 f | 0.844 f | 37.3 d | 39.7 ab |
| 21D | Control | 0.78 e | 0.80 a | 0.179 b | 0.191 a | 0.256 ab | 0.180 a | 0.744 g | 0.820 ij | 39.8 b | 40.5 a |
| | Control + MeJA | 0.78 e | 0.80 a | 0.184 b | 0.190 a | 0.262 a | 0.177 a | 0.748 g | 0.823 i | 40.1 b | 40.2 a |
| | Al | 0.79 bc | 0.76 f | 0.088 g | 0.120 f | 0.130 gh | 0.167 b | 0.870 b | 0.833 g | 23.2 f | 26.1 de |
| | Al + MeJA | 0.79 c | 0.80 c | 0.164 cd | 0.175 b | 0.184 d | 0.178 a | 0.816 d | 0.822 ij | 35.6 e | 38.1 a |
| | WD | 0.78 de | 0.75 hi | 0.065 j | 0.076 g | 0.083 h | 0.132 f | 0.917 b | 0.868 e | 14.1 j | 16.4 g |
| | WD + MeJA | 0.79 d | 0.80 c | 0.178 bc | 0.128 e | 0.252 b | 0.173 ab | 0.748 g | 0.827 h | 38.7 c | 27.8 d |
| | Al + WD | 0.79 d | 0.75 h | 0.082 h | 0.129 e | 0.139 g | 0.157 d | 0.861 b | 0.843 f | 17.9 hi | 27.9 d |
| | Al + WD + MeJA | 0.79 bc | 0.79 cd | 0.171 c | 0.179 b | 0.242 c | 0.162 c | 0.758 f | 0.838 fg | 37.3 d | 38.9 ab |

Stomatal conductance ranged from 0.03 to 0.22 mol $H_2O$ $m^{-2}$ $s^{-1}$, while leaf transpiration (E) varied between 0.8 and 4.5 mmol $H_2O$ $m^{-2}$ $s^{-1}$ (Figure 6B,C). Both parameters showed high sensitivity to the type of stress applied, with WD exerting the strongest effect on stomatal regulation and gas exchange. The magnitude of stress impact followed the same pattern observed for An (WD > Al + WD > Al). WD reduced gs and E by 40–60% relative to the control, whereas combined stress and Al alone produced more moderate decreases of up to 25% (Figure 6B,C). These results indicate that water limitation, rather than Al toxicity, was the main driver of stomatal closure and reduced gas exchange in both cultivars. Exogenous MeJA significantly improved gs and E under all stress conditions (Figure 6B,C). In Al + MeJA, gs increased by 25–35% and E by 20–35% relative to Al. Under WD, the recovery was stronger, with gs increasing by 50–60% and E by up to 55% compared with WD. Under combined stress (Al + WD + MeJA), gs and E also recovered markedly, with increases of approximately 50% and 30–45%, respectively. In most cases, MeJA restored values close to the control, although WD + MeJA remained slightly lower. The Control + MeJA treatment showed small increases (5–10%), suggesting

a basal stimulatory effect of jasmonate under non-stressed conditions. Cultivar responses differed markedly. Star exhibited higher gs and E under optimal conditions but showed greater sensitivity to stress, with reductions exceeding 60% under WD and Al + WD. In contrast, Legacy maintained more stable values and showed a more effective recovery after MeJA application, frequently reaching control levels (Figure 6B,C).

When calculating intrinsic water use efficiency (WUEi = An/gs) and apparent water use efficiency (WUE = An/E), significant differences were observed depending on the treatment, cultivar, and their interaction ($p < 0.001$) (Table 1). For WUEi, values ranged from 8 to 50 μmol $CO_2$ $mol^{-1}$ $H_2O$, with no defined temporal trend, but similar to the previous parameters. Compared with the control, the Al treatment produced slight variations in WUEi, with values close to those of the control (ca. 10%). In contrast, WD caused the largest fluctuations, with both increases and decreases exceeding 50%, while combined stress (Al + WD) showed intermediate changes of 10–20% (Table 1). The MeJA application significantly stabilized the An/gs ratio and reduced stress-induced variability. In Al + MeJA, WUEi increased by 10–20% compared to Al, WD + MeJA showed the most evident recovery (15–30%), and Al + WD + MeJA increased by 10–25% compared to Al + WD, often reaching or exceeding control values. Comparative analysis between cultivars revealed marked differences in WUEi stability. The Star cultivar showed moderate control values and much wider fluctuations under stress, reflecting more unstable stomatal regulation. In contrast, Legacy maintains more consistent values close to the control (Table 1).

Apparent WUE ranged from 0.5 to 5 μmol $CO_2$ $mmol^{-1}$ $H_2O$ (Table 1). Unlike WUEi, the greatest fluctuations were observed under stress, particularly in the Star cultivar, indicating high sensitivity of this parameter. Compared with the control, Al caused the greatest reduction in WUE (ca. 50%), followed by combined stress (Al + WD; ca. 45%), whereas WD produced a more moderate decline (ca. 30%). Exogenous MeJA markedly improved WUE under all stress conditions. WUE increased by more than 50% in Al + MeJA relative to Al, and by 30–45% in WD + MeJA and Al + WD + MeJA compared with their respective stress treatments. Clear cultivar differences were observed. Legacy maintained higher and more stable WUE across treatments and sampling times, whereas Star showed lower baseline values and stronger fluctuations, with reductions reaching 60% under Al and Al + WD (Table 1).

Photosystem II (PSII) fluorescence parameters were analyzed, including Fv/Fm, effective quantum efficiency (ΦPSII), qP, qN, and ETR. All variables showed significant differences among treatments, sampling times, cultivars, and their interactions ($p < 0.05$) (Table 2). Overall, the fluorescence responses indicated a clear sensitivity of the photosynthetic apparatus to abiotic stress, following the pattern WD > Al + WD > Al. A consistent recovery after MeJA application. Maximum quantum efficiency showed optimal values close to 0.80 in the control treatments of both cultivars. Stress treatments caused moderate reductions: Al decreased Fv/Fm by about 6%, whereas WD and Al + WD reduced it by approximately 9% relative to the control. The reductions were more pronounced in Star, which reached the lowest value (0.74), while Legacy maintained more stable values (ca. 0.78). Application of MeJA (Al + MeJA, WD + MeJA, Al + WD + MeJA) restored Fv/Fm to values close to the control (ca. 0.79), indicating recovery of PSII photochemical efficiency (Table 2).

The effective quantum efficiency of photosystem II (ΦPSII) ranged from 0.058 to 0.201. Under control conditions, mean values were 0.184 in Legacy and 0.166 in Star, consistent with high photosynthetic activity. Stress treatments caused pronounced reductions in ΦPSII. WD produced the strongest effect, decreasing ΦPSII by 60% in Legacy and 65% in Star. Combined stress (Al + WD) also reduced values by 45–55%, whereas Al alone caused smaller decreases of 33% in Legacy and 55% in Star relative to the control. Exogenous MeJA

significantly increased ΦPSII under all stress conditions. In Al + MeJA, values increased by 25–35% relative to Al. Under WD + MeJA, ΦPSII recovered to levels close to the control, while Al + WD + MeJA improved values by about 40% compared with the combined stress without MeJA. Across cultivars, Legacy consistently maintained higher and more stable ΦPSII values and fully recovered with MeJA. In contrast, Star exhibited greater sensitivity and wider fluctuations, with the strongest reductions under WD and Al + WD (Table 2).

Photochemical quenching ranged from 0.082 to 0.263, reflecting variability in the proportion of open PSII reaction centers among treatments. Under control conditions, mean values were higher in Legacy (0.252) than in Star (0.176), indicating a greater basal photochemical efficiency in Legacy. Stress treatments reduced qP, with WD producing the strongest decreases of about 60% in Legacy and 50% in Star. Combined stress reduced by around 40% in both cultivars, while Al alone decreased qP by approximately 40% in Legacy and 50% in Star. Application of MeJA promoted substantial recovery of qP. The values increased by about 30% in Al + MeJA and Al + WD + MeJA relative to Al, whereas WD + MeJA restored qP to levels similar to or higher than the control. Across treatments, Legacy maintained consistently higher qP values than Star and showed a more complete recovery after MeJA application.

Non-photochemical quenching showed an opposite pattern, ranging from 0.744 to 0.918 and increasing under stress conditions. Control values were 0.749 in Legacy and 0.823 in Star. Stress treatments increased qN by 16% in Legacy and 8% in Star under Al, by about 20% under WD, and by approximately 15% under combined stress. In contrast to the other fluorescence parameters, MeJA reduced qN under both individual and combined stress, restoring qN values close to those of the control. Although Star exhibited higher basal qN values, Legacy showed stronger relative activation and a more efficient response to MeJA (Table 2).

Under control conditions, average ETR values were approximately 40 μmol $e^{-}$ $m^{-2}$ $s^{-1}$, with no significant differences between cultivars, indicating efficient electron transport and high PSII activity. Stress treatments reduced ETR following the same pattern observed for the other fluorescence parameters (WD > Al + WD > Al). WD caused the strongest declines, reducing ETR by up to 55% in Legacy and 65% in Star. Combined stress produced similar decreases of about 50% in Legacy and 65% in Star, whereas Al alone caused more moderate reductions of approximately 35% in Legacy and 50% in Star.

MeJA significantly improved ETR under stress. In Al + MeJA and Al + WD + MeJA, ETR increased by up to 45% relative to Al, while WD + MeJA produced the strongest recovery, with values exceeding those of the control. Consistent with the other fluorescence parameters (Fv/Fm, ΦPSII, and qP), Legacy maintained higher ETR values than Star across treatments, averaging about 20% greater values and showing a more effective recovery after MeJA application (Table 2).

To support the results for photosynthesis and fluorescence, the content and proportions of photosynthetic pigments were analyzed in leaves of *V. corymbosum* (cultivars Legacy and Star), including chlorophyll a, chlorophyll b, carotenoids, and the ratios Chl a/b and Chl/Car (Figure 7 and Tables 3 and 4). Significant differences were observed among treatments, cultivars, sampling times, and their interactions ($p < 0.001$ for chlorophylls and $p < 0.05$ for carotenoids). Overall, stress treatments caused marked reductions in chlorophyll content accompanied by relative increases in carotenoids and activation of the xanthophyll cycle, particularly in the Legacy cultivar. No clear temporal trends were observed. Instead, responses were mainly associated with stress intensity, following the pattern Al + WD > WD > Al.

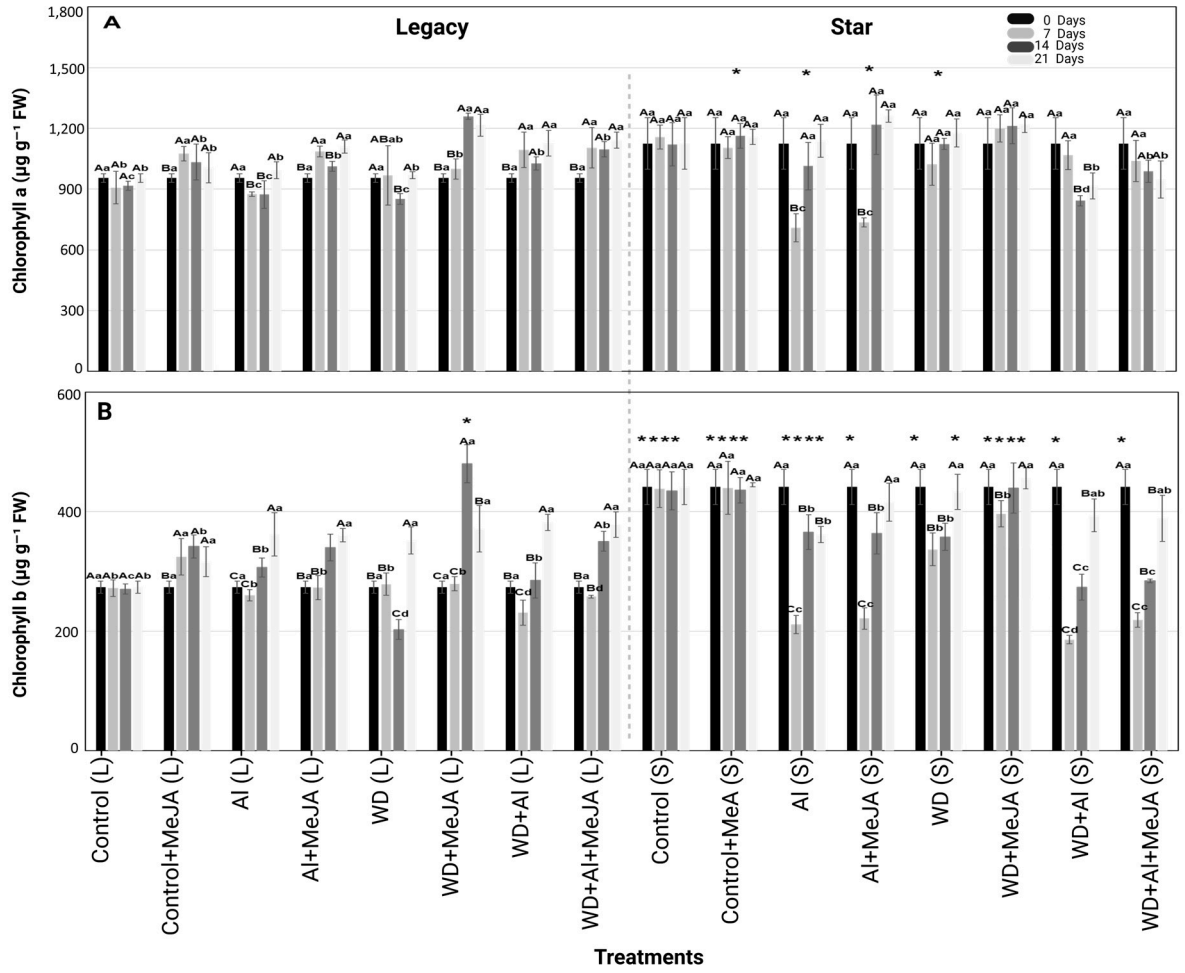


**Figure 7.** Quantification of pigments on leaves of *V. corymbosum* L. cultivars Legacy and Star, under conditions of combined stress (Al + WD) and application of MeJA. (**A**) Chlorophyll a. (**B**) Chlorophyll b. Treatments included: Control, Aluminum (Al), WD, and combinations with MeJA (Control + MeJA, Al + MeJA, WD + MeJA, Al + WD + MeJA). Different capital letters indicate significant differences among times within each cultivar and treatment (ANOVA, Tukey HSD, $p < 0.05$). Different lower case letter indicate significant differences among treatments with each cultivar and time (ANOVA, Tukey HSD, $p < 0.05$). Asterisks (*) indicate significant differences between cultivars for the same treatment and time.

Chlorophyll a and b concentrations showed contrasting responses between cultivars under stress and MeJA application (Figure 7). In Legacy, chlorophyll a remained relatively stable across treatments and evaluation times, with reductions generally low about 10 to 15% relative to the control (Figure 7A). The lowest values were observed under WD conditions, whereas MeJA maintained or slightly increased chlorophyll a under WD + MeJA and WD + Al + MeJA treatments. In contrast, Star showed higher basal chlorophyll a levels than Legacy. Still, there was also a stronger decrease in pigment under stress conditions (Figure 7A). Aluminum stress reduced chlorophyll a by approximately 20–25%, while WD and WD + Al caused reductions close to 30–40% relative to the control. MeJA partially restored chlorophyll a levels under WD + MeJA conditions, although this effect was less consistent under combined stress treatments. Overall, Legacy maintained greater pigment stability, whereas Star showed higher sensitivity to stress progression (Figure 7A). In Legacy, chlorophyll b values remained relatively stable across treatments. However, MeJA increased pigment concentration by approximately 10–20% under WD + MeJA and WD + Al + MeJA relative to the corresponding stress treatments (Figure 7B). In contrast, Star showed marked

reductions in chlorophyll b under stress conditions. Aluminum stress reduced chlorophyll b by approximately 25–35%, whereas WD and WD + Al caused reductions of 40–50% relative to the control. The lowest values were observed under WD + Al conditions at 7 days. Therefore, Star exhibited the greatest decline in chlorophyll b, whereas Legacy maintained greater pigment stability throughout stress treatments (Figure 7B).

**Table 3.** Ratio of chlorophyll a to chlorophyll b and total chlorophylls to total carotenoids *V. corymbosum* L. cultivars Legacy and Star, under conditions of combined stress (Al + WD) and application of MeJA. Treatments included: Control, Aluminum (Al), WD, and combinations with MeJA (Control + MeJA, Al + MeJA, WD + MeJA, Al + WD + MeJA). Different capital letters indicate significant differences among times within each cultivar and treatment (ANOVA, Tukey HSD, $p < 0.05$). Different lower case letter indicate significant differences among treatments with each cultivar and time (ANOVA, Tukey HSD, $p < 0.05$). Asterisks (*) indicate significant differences between cultivars for the same treatment and time.

| | | Chll a/Chll b | | Chll/Car | |
|---|---|---|---|---|---|
| **Time** | **Treatments** | **Legacy** | **Star** | **Legacy** | **Star** |
| 7D | Control | 3.3 Ab * | 2.6 Ac | 3.9 Aab * | 3.5 Ab |
| | Control + MeJA | 3.3 Ab * | 2.5 Ac | 4.5 Aa * | 3.2 Ab |
| | Al | 3.4 Ab | 3.4 Ab | 2.6 Ac | 3.8 Aab * |
| | Al + MeJA | 4.0 Aab * | 3.3 Ab | 3.1 Ab | 3.7 Aab * |
| | WD | 3.5 Ab * | 3.0 Ab | 3.7 Aab | 3.8 Aab |
| | WD + MeJA | 3.6 Ab * | 3.0 Ab | 3.6 Aab | 3.9 Aa * |
| | Al + WD | 4.7 Aa | 5.8 Aa * | 3.5 Aab | 3.6 Ab |
| | Al + WD + MeJA | 4.3 Aa | 4.7 Aa * | 3.6 Aab * | 3.3 Ab |
| 14D | Control | 3.4 Ab * | 3.1 Ab | 4.0 Aab * | 3.4 Ab |
| | Control + MeJA | 3.0 Ab * | 2.6 Ac | 4.5 Aa * | 3.4 Ab |
| | Al | 2.9 Ab * | 2.7 Ac | 2.6 Ac | 3.4 Ab * |
| | Al + MeJA | 3.0 Ab * | 2.8 Ac | 3.1 Ab | 3.7 Aab * |
| | WD | 4.2 Aa * | 3.3 Ab | 4.7 Aa * | 4.1 Aa |
| | WD + MeJA | 2.6 Bb | 3.2 Ab * | 3.7 Aab | 3.9 Aa |
| | Al + WD | 3.6 Aab * | 2.8 Ac | 3.6 Ab * | 2.8 Bb |
| | Al + WD + MeJA | 3.1 Ab | 3.1 Ab | 3.8 Aab * | 2.9 Bb |
| 21D | Control | 3.5 Ab * | 2.6 Ac | 4.1 Aab * | 3.4 Ab |
| | Control + MeJA | 3.2 Ab * | 2.6 Ac | 4.3 Aa * | 3.4 Ab |
| | Al | 2.8 Ab | 3.2 Ab * | 3.8 Aab * | 3.5 Ab |
| | Al + MeJA | 3.1 Ab * | 3.0 Ab | 4.1 Aab * | 3.6 Ab |
| | WD | 2.8 Bb | 2.7 Ac | 4.1 Aab * | 3.9 Aa |
| | WD + MeJA | 3.3 Ab * | 2.7 Ac | 4.4 Aa * | 3.8 Aa |
| | Al + WD | 3.0 Ab | 3.6 Aa * | 2.8 Bc | 2.9 Bb |
| | Al + WD + MeJA | 3.0 Ab | 3.3 Aab | 2.9 Bb | 2.9 Bb |

**Table 4.** Quantification of carotenoids on leaves of *V. corymbosum* L. cvs. Legacy and Star, under conditions of combined stress (Al + WD) and application of MeJA. Treatments included: Control, Aluminum (Al), WD, and combinations with MeJA (Control + MeJA, Al + MeJA, WD + MeJA, Al + WD + MeJA). Different lower case letters indicate significant differences between treatments within each cultivar and time (ANOVA, Tukey HSD, $p < 0.05$).

| | | Legacy | | | | | Star | | | | |
|---|---|---|---|---|---|---|---|---|---|---|---|
| **Time** | **Treatments** | **Beta Carotene** | **Lutein** | **Neoxanthin** | **Violaxanthin** | **Anteraxanthin** | **Beta Carotene** | **Lutein** | **Neoxanthin** | **Violaxanthin** | **Anteraxanthin** |
| 7D | Control | 58.7 c | 122.1 d | 53.0 d | 63.4 d | 6.5 e | 66.3 a | 193.3 a | 76.1 b | 113.7 a | 11.1 b |
| | Control + MeJA | 60.9 bc | 126.8 d | 51.3 d | 66.1 d | 6.3 e | 67.1 a | 204.5 a | 81.0 ab | 116.2 a | 11.3 b |
| | Al | 82.1 a | 183.3 a | 82.6 b | 89.3 b | 9.1 c | 44.0 c | 91.6 f | 46.0 f | 51.1 d | 10.8 b |
| | Al + MeJA | 85.3 a | 187.3 a | 80.3 b | 68.6 d | 10.7 c | 45.5 c | 98.2 f | 45.5 f | 56.3 d | 10.7 b |
| | WD | 44.4 de | 143.7 c | 46.0 e | 89.2 b | 9.2 c | 68.2 a | 155.6 d | 57.5 e | 64.7 c | 16.2 a |
| | WD + MeJA | 57.2 c | 148.5 b | 54.8 d | 85.4 b | 13.6 b | 73.8 a | 174.2 b | 68.3 c | 77.9 bc | 16.2 a |
| | Al + WD | 39.3 e | 170.5 ab | 77.7 b | 75.1 c | 15.7 b | 62.7 ab | 140.8 e | 68.6 c | 65.5 c | 12.9 ab |
| | Al + WD + MeJA | 51.9 d | 167.4 ab | 84.7 b | 65.5 d | 15.0 b | 66.7 a | 153.4 d | 70.7 c | 73.7 b | 12.9 ab |
| 14D | Control | 56.3 c | 119.9 d | 51.0 d | 62.0 d | 6.4 e | 65.3 a | 198.1 a | 75.0 bc | 111.3 a | 12.2 b |
| | Control + MeJA | 64.2 bc | 121.5 d | 51.1 d | 65.0 d | 6.4 e | 67.4 a | 196.0 a | 85.9 a | 110.6 a | 11.5 b |
| | Al | 61.3 b | 193.9 a | 91.6 ab | 101.3 a | 13.6 b | 61.7 ab | 183.9 ab | 68.4 c | 80.2 b | 10.7 b |
| | Al + MeJA | 80.7 a | 195.5 a | 91.9 ab | 72.1 bc | 14.1 b | 66.5 a | 191.6 a | 81.6 a | 80.3 b | 10.9 b |
| | WD | 40.2 e | 82.6 e | 47.6 e | 44.5 e | 9.9 c | 56.6 b | 159.9 d | 64.8 d | 65.5 c | 13.0 b |
| | WD + MeJA | 62.6 bc | 175.7 ab | 105.9 a | 103.4 a | 19.3 a | 65.5 a | 185.0 ab | 79.1 b | 75.9 b | 14.1 ab |
| | Al + WD | 48.9 d | 155.5 b | 81.7 b | 64.7 d | 14.8 b | 68.7 a | 171.7 b | 82.4 a | 69.6 bc | 13.6 ab |
| | Al + WD + MeJA | 59.5 b | 151.9 b | 84.6 b | 71.2 bc | 18.8 a | 68.3 a | 179.9 b | 83.4 a | 79.5 b | 13.6 ab |
| 21D | Control | 55.7 c | 120.7 d | 54.0 d | 62.6 d | 6.2 e | 66.3 a | 196.8 a | 73.3 bc | 111.4 a | 11.6 b |
| | Control + MeJA | 65.2 bc | 121.2 d | 51.6 d | 62.7 d | 6.4 e | 68.3 a | 201.3 a | 84.2 a | 111.1 a | 11.1 b |
| | Al | 63.9 b | 143.6 c | 68.1 c | 74.3 c | 12.9 bc | 61.6 ab | 175.0 b | 73.6 bc | 104.3 a | 8.6 c |
| | Al + MeJA | 84.8 a | 149.5 b | 68.9 c | 67.6 d | 18.1 a | 66.7 a | 185.6 ab | 78.2 b | 106.7 a | 10.8 b |
| | WD | 45.5 e | 141.7 c | 60.4 c | 62.0 d | 8.3 cd | 55.0 b | 181.0 ab | 69.6 c | 100.1 a | 6.9 d |
| | WD + MeJA | 63.4 b | 137.8 c | 61.0 c | 78.5 c | 5.3 e | 64.2 a | 197.1 a | 80.9 ab | 100.7 a | 8.5 c |
| | Al + WD | 61.2 b | 156.6 b | 65.8 c | 62.5 d | 7.9 d | 67.8 a | 196.2 a | 84.2 a | 103.9 a | 7.5 d |
| | Al + WD + MeJA | 64.0 b | 151.4 b | 70.0 c | 63.1 d | 13.6 b | 67.8 a | 202.3 a | 83.6 a | 102.0 a | 12.5 ab |

The chlorophyll a/b ratio ranged from 2.5 to 4.1 and showed significant variation depending on stress conditions and MeJA application (Table 3). Under control conditions, mean values were 3.5 in Legacy and 2.5 in Star. Stress treatments reduced this ratio, with the largest decreases under Al + WD (up to 25%), followed by WD (around 20%) and Al (approximately 10%). The exogenous application of MeJA increased the Chl a/b ratio by 20–30% relative to the respective stress treatments, restoring it to values close to those of the control. Across treatments, Legacy maintained consistently higher Chl a/b values than Star. Similarly, the ratio between total chlorophylls and carotenoids (Chl/Car) ranged from 2.6 to 5.8 and showed significant variation among treatments and cultivars (Table 3). Under control conditions, values averaged 4.0 in Legacy and 3.4 in Star. Combined stress reduced the Chl/Car ratio by 15–20% in both cultivars. Under WD, Legacy showed moderate increases of about 10%, whereas Star remained close to control values. In the Al stress condition, contrasting responses were observed between cultivars, with a reduction of about 20% in Legacy and an increase of up to 60% in Star. The exogenous application of MeJA restored Chl/Car values to levels close to those of the control in Legacy, whereas Star continued to show greater variability. Overall, Legacy maintained higher and more stable Chl/Car ratios than Star, indicating greater stability of the photosynthetic apparatus under stress (Table 3).

Accessory carotenoids were quantified because of their roles in photochemical protection and antioxidant responses to abiotic stress. The pigments β-carotene, lutein, neoxanthin, violaxanthin, and antheraxanthin showed significant differences among treatments, cultivars, and their interaction ($p < 0.05$) (Table 4). β-carotene content differed significantly among treatments, ranging from 40 to 85 μg $g^{-1}$ FW in Legacy and from 40 to 75 μg $g^{-1}$ FW in Star. Under control conditions, both cultivars showed similar concentrations of approximately 60 μg $g^{-1}$ FW. Under $Al^{3+}$ stress, the response differed between cultivars: β-carotene increased by up to 40% in Legacy but decreased by about 35% in Star compared with the control. Under combined stress (Al + WD), concentrations initially declined but stabilized toward the end of the experimental period, remaining about 10% below control levels. Meanwhile, WD alone decreased β-carotene levels in both cultivars, with reductions of up to 30% in Legacy and 20% in Star. Exogenous application of MeJA stimulated β-carotene biosynthesis. In WD + MeJA, concentrations increased by approximately 40% compared with WD, while in Al + WD + MeJA, the increase reached about 30%. In contrast, Al + MeJA treatments maintained β-carotene levels close to those observed under control conditions. Across treatments, Legacy generally maintained β-carotene concentrations 10–20% higher than Star, indicating greater stability of carotenoid metabolism under stress conditions (Table 4).

Lutein content also showed significant differences among treatments, ranging from 80 to 200 μg $g^{-1}$ FW depending on stress conditions and MeJA application (Table 4). Under control conditions, the Legacy and Star cultivars showed average concentrations of 122 and 193 μg $g^{-1}$ FW, respectively. Under $Al^{3+}$ stress, the responses differed between cultivars. In Legacy, lutein increased significantly, reaching values 40–60% higher than the control, whereas in Star, concentrations decreased by up to 50%. Under combined stress (Al + WD), intermediate responses were observed, with lutein increased by up to 30% in Legacy but decreased by about 20% in Star. WD alone caused temporary fluctuations in Legacy, whereas in Star, lutein remained consistently lower, with reductions of approximately 20% compared with the control. Exogenous MeJA promoted recovery of lutein levels in both cultivars, restoring concentrations to values similar to or higher than those observed under control conditions. Across treatments, Legacy showed greater stability in lutein content, whereas Star exhibited higher basal levels, stronger declines under stress, and greater overall variability (Table 4).

Neoxanthin content showed significant differences among treatments, ranging from 45 to 110 μg $g^{-1}$ FW in Legacy and from 45 to 90 μg $g^{-1}$ FW in Star (Table 4). Under control conditions, the Legacy and Star cultivars presented average concentrations of 53 and 76 μg $g^{-1}$ FW, respectively. Under $Al^{3+}$ stress, contrasting responses were observed between cultivars. In Legacy, neoxanthin increased markedly, reaching values 40–80% higher than the control, whereas in Star, concentrations initially decreased by approximately 40%. Under combined stress (Al + WD), Legacy maintained relatively high and stable levels (20–30% above control values), while Star showed intermediate responses, approaching control levels toward the end of the experimental period. WD alone caused moderate decreases in neoxanthin in both cultivars, which were more pronounced in Star (20–25%) than in Legacy (10–15%). Exogenous MeJA application significantly modulated neoxanthin accumulation. In Legacy, MeJA promoted a strong recovery under WD, with increases of 50–120% compared with WD, while under combined stress, moderate increases of approximately 10% were observed relative to Al + WD. In contrast, Al + MeJA treatments maintained neoxanthin concentrations close to those observed under $Al^{3+}$ stress alone. In Star, MeJA induced partial recovery under all stress conditions, with increases of 10–20% compared with treatments without MeJA, although values did not fully reach control levels (Table 4).

Xanthophyll pigments associated with the VAZ cycle were quantified, and violaxanthin showed significant variation among treatments, ranging from 40 to 120 μg $g^{-1}$ FW depending on stress conditions and MeJA application (Table 4). Under control conditions, the Legacy and Star cultivars presented average values of approximately 60 and 110 μg $g^{-1}$ FW, respectively. Under $Al^{3+}$ stress, contrasting responses were observed between cultivars. In Legacy, violaxanthin increased consistently relative to the control, reaching values up to 60% higher. In contrast, Star showed a sustained decrease of up to 50% compared with the control, with the strongest reduction occurring during the early stages of the experiment. Under WD and combined stress (Al + WD), cultivar-specific responses were also observed. In Legacy, violaxanthin initially increased (approximately 40% relative to the control) and later stabilized near control levels toward the end of the experimental period. In contrast, WD consistently reduced violaxanthin levels in Star, resulting in decreases of up to 40% compared with the control. Exogenous MeJA application modulated violaxanthin accumulation in both cultivars. In Legacy, MeJA reduced the $Al^{3+}$-induced overaccumulation (up to 20% relative to Al). Under WD + MeJA, violaxanthin increased markedly, ranging from 20% to 130% compared with WD, depending on the sampling time, restoring levels close to or above those of the control. Under combined stress (Al + WD + MeJA), moderate increases of approximately 10% were observed compared with Al + WD. In Star, MeJA promoted partial recovery under all stress conditions, with increases of up to 10% under Al + MeJA, 20% under WD + MeJA, and 15% under Al + WD + MeJA relative to the respective stress treatments without MeJA, although values did not consistently reach control levels (Table 4).

Antheraxanthin content showed significant differences among treatments, ranging from 5.3 to 19.3 μg $g^{-1}$ FW in Legacy and from 6.9 to 16.2 μg $g^{-1}$ FW in Star (Table 4). Under control conditions, the Legacy and Star cultivars presented average values of 6.4 and 11.6 μg $g^{-1}$ FW, respectively. Combined stress (Al + WD) produced the largest increases in antheraxanthin, reaching approximately 130% above control values in Legacy and 15% in Star. Under $Al^{3+}$ stress, Legacy showed sustained increases of 40–110% relative to the control, whereas Star showed moderate decreases. WD alone induced moderate increases in Legacy (up to 55%). In contrast, Star showed a more variable response, with an initial increase of approximately 45% followed by a decrease of up to 40% toward the end of the experimental period. The exogenous application of MeJA increased antheraxanthin levels

under all stress conditions. In Legacy, the strongest stimulation occurred under WD (95% vs. WD), followed by combined stress (40% vs. Al + WD) and $Al^{3+}$ stress (30% vs. Al). In Star, MeJA produced more moderate increases, generally between 10% and 20%, mainly under WD and combined stress. Across treatments, Star exhibited higher basal levels of antheraxanthin but greater temporal variability, whereas Legacy showed more consistent increases under stress conditions (Table 4).

### *3.4. Antioxidant Response in Vaccinium corymbosum L. Under Aluminum Stress and Water Deficit*

Lipid peroxidation (LP) showed highly significant differences among treatments, cultivars, and their interaction ($p < 0.001$) (Figure 8A). Lipid peroxidation values ranged from 35 to 230 nmol $g^{-1}$ FW, reflecting strong variation depending on stress conditions and MeJA application. Under control conditions, both cultivars showed similar baseline levels, with average values close to 50 nmol $g^{-1}$ FW. All stress treatments significantly increased LP concentration. Under $Al^{3+}$ stress, LP levels increased by 140–160% in Legacy and by 180–210% in Star compared with the control. WD produced an even stronger effect, with increases of 200–250% in both cultivars. Combined stress (Al + WD) further intensified lipid peroxidation, reaching increases of up to 240% in Legacy and 270% in Star relative to control plants. Overall, LP accumulation was consistently higher under WD and combined stress than under $Al^{3+}$ alone, indicating a stronger contribution of dehydration to oxidative damage in leaf tissues (Figure 8A). Exogenous MeJA application significantly reduced LP concentrations under all stress treatments (Figure 8A). Under $Al^{3+}$ stress (Al + MeJA), LP levels decreased by 30–45% in Legacy and 25–35% in Star compared with Al alone. Under WD (WD + MeJA), the reduction was more pronounced, reaching 40–55% in Legacy and 30–40% in Star. Under combined stress (Al + WD + MeJA), LP concentrations also declined substantially, by 30–40% in Legacy and 25–35% in Star relative to Al + WD. Across treatments, Legacy consistently maintained lower LP levels than Star, with differences ranging from 15% to 30%. In addition, the reduction promoted by MeJA was generally more pronounced in Legacy, particularly under WD, whereas Star showed greater variability and a less complete recovery of LP levels (Figure 8A).

Lipid peroxidation in roots showed significant differences among treatments, cultivars, and their interaction ($p < 0.001$) (Figure 9B). LP values ranged from 20 to 150 nmol $g^{-1}$ FW, indicating lower oxidative damage than that observed in leaves but with a response strongly dependent on stress conditions and MeJA application. Under control conditions, Legacy and Star showed low basal LP levels (28.4 $\pm$ 3.1 and 34.1 $\pm$ 2.9 nmol $g^{-1}$ FW, respectively), with no significant differences between cultivars. Aluminum stress significantly increased LP concentration, reaching increases of 110–130% in Legacy and 130–170% in Star relative to the control. WD produced even greater increases in lipid peroxidation, with LP rising by 120–150% in Legacy and 140–170% in Star. Combined stress (Al + WD) resulted in the highest LP accumulation in roots for both cultivars, exceeding 200% of control values (Figure 9B). Exogenous MeJA application reduced LP concentrations in roots under all stress treatments (Figure 8B). In Al + MeJA, LP levels decreased by 25–35% compared with Al alone. Under WD + MeJA, reductions ranged from 30 to 40%, while under combined stress (Al + WD + MeJA), LP decreased by 25–35%. The mitigation effect was generally more pronounced in the Legacy cultivar. In several treatments, LP concentrations approached baseline levels after 21 days, suggesting partial recovery of the antioxidant status in root tissues. Across treatments, Star consistently showed LP values 15–25% higher than those observed in Legacy and exhibited greater temporal variability.

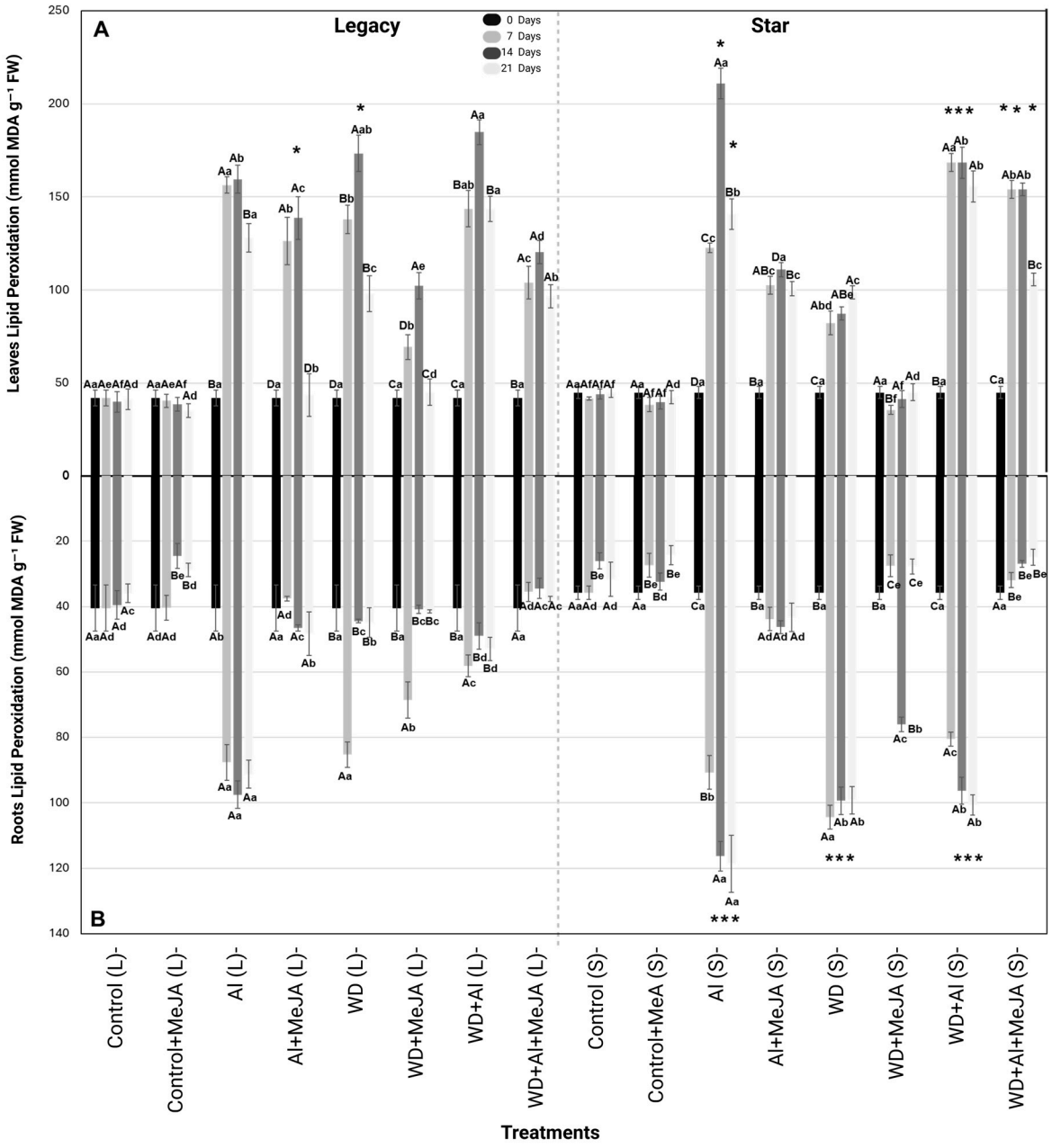


**Figure 8.** Lipid peroxidation of *V. corymbosum* L. cultivars Legacy and Star, under conditions of combined stress (Al + WD) and application of MeJA. (**A**) Leaves. (**B**) Roots. Treatments included: Control, Aluminum (Al), WD, and combinations with MeJA (Control + MeJA, Al + MeJA, WD + MeJA, Al + WD + MeJA). Different capital letters indicate significant differences among times within each cultivar and treatment (ANOVA, Tukey HSD, $p < 0.05$). Different lower case letter indicate significant differences among treatments with each cultivar and time (ANOVA, Tukey HSD, $p < 0.05$). Asterisks (*) indicate significant differences between cultivars for the same treatment and time.

The activation of the antioxidant system in both cultivars was evaluated in response to oxidative stress induced by abiotic stresses and by exogenous MeJA application. Antioxidant activity, total phenols, and SOD activity showed significant differences among treatments, cultivars, sampling times, and their interactions ($p < 0.001$) (Figures 9 and 10). In general, antioxidant activity was higher in leaves (Figure 9) than in roots (Figure 10), which may be associated with the previously observed greater lipid peroxidation in leaf tissues. In addition, antioxidant-related parameters tended to increase under stress conditions and after MeJA application in both cultivars (Figure 9). Antioxidant activity was 2–4 times

higher in leaves (Figure 9) than in roots (Figure 10). Antioxidant activity also increased over time, reaching maximum values at 21 days, particularly in treatments with MeJA such as WD + MeJA and Al + WD + MeJA (Figures 9A and 10A).

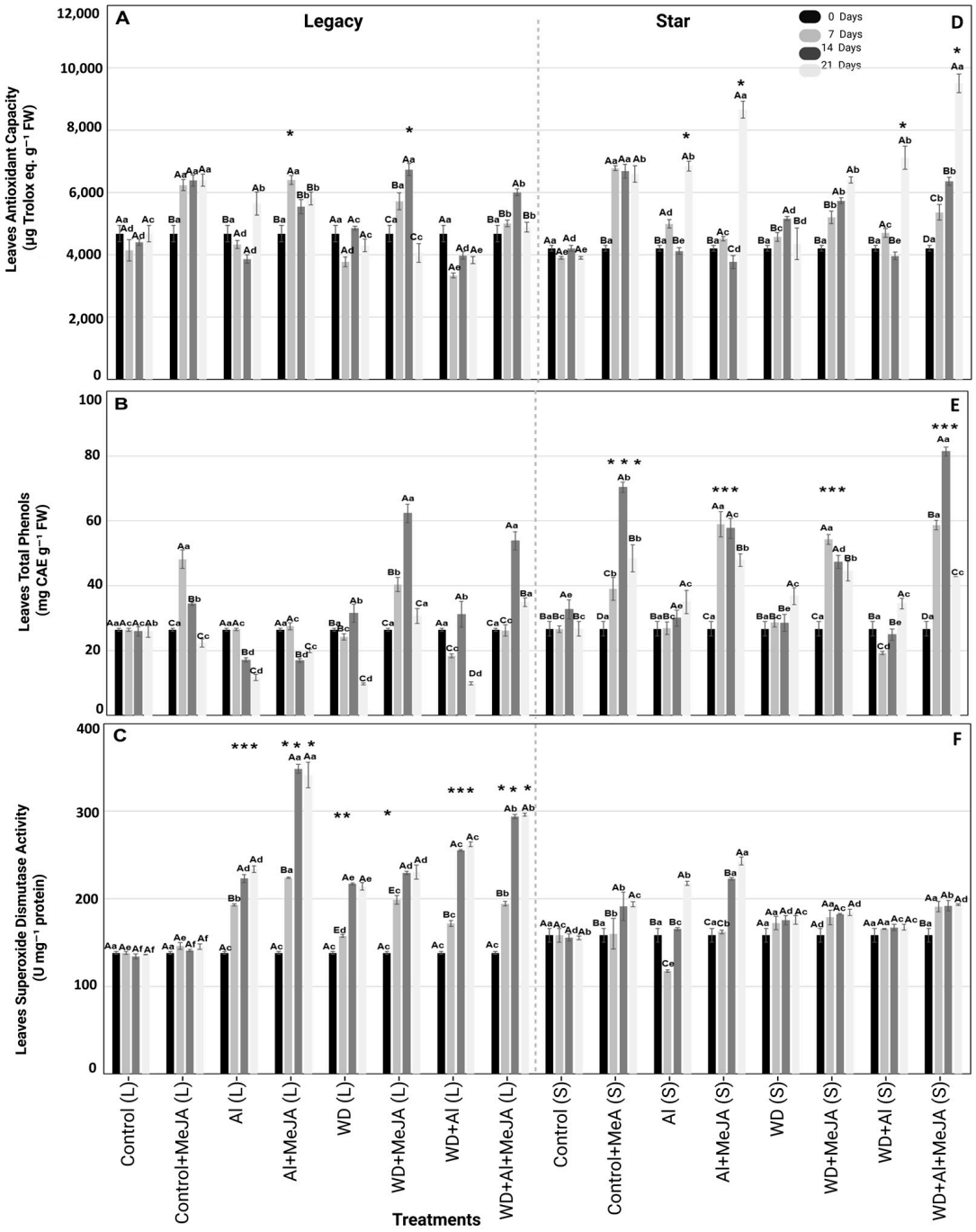


**Figure 9.** Leaves antioxidant response of *V. corymbosum* L. cultivars Legacy and Star, under combined stress (Al + WD) and application of MeJA. (**A,D**) Antioxidant Activity, (**B,E**) Total Phenols, (**C,F**) SOD activity. Treatments included: Control, Aluminum (Al), WD, and combinations with MeJA (Control + MeJA, Al + MeJA, WD + MeJA, Al + WD + MeJA). Different capital letters indicate significant differences among times within each cultivar and treatment (ANOVA, Tukey HSD, $p < 0.05$). Different lower case letters indicate significant differences among treatments within each cultivar and time (ANOVA, Tukey HSD, $p < 0.05$). Asterisks (*) indicate significant differences between cultivars for the same treatment and time.

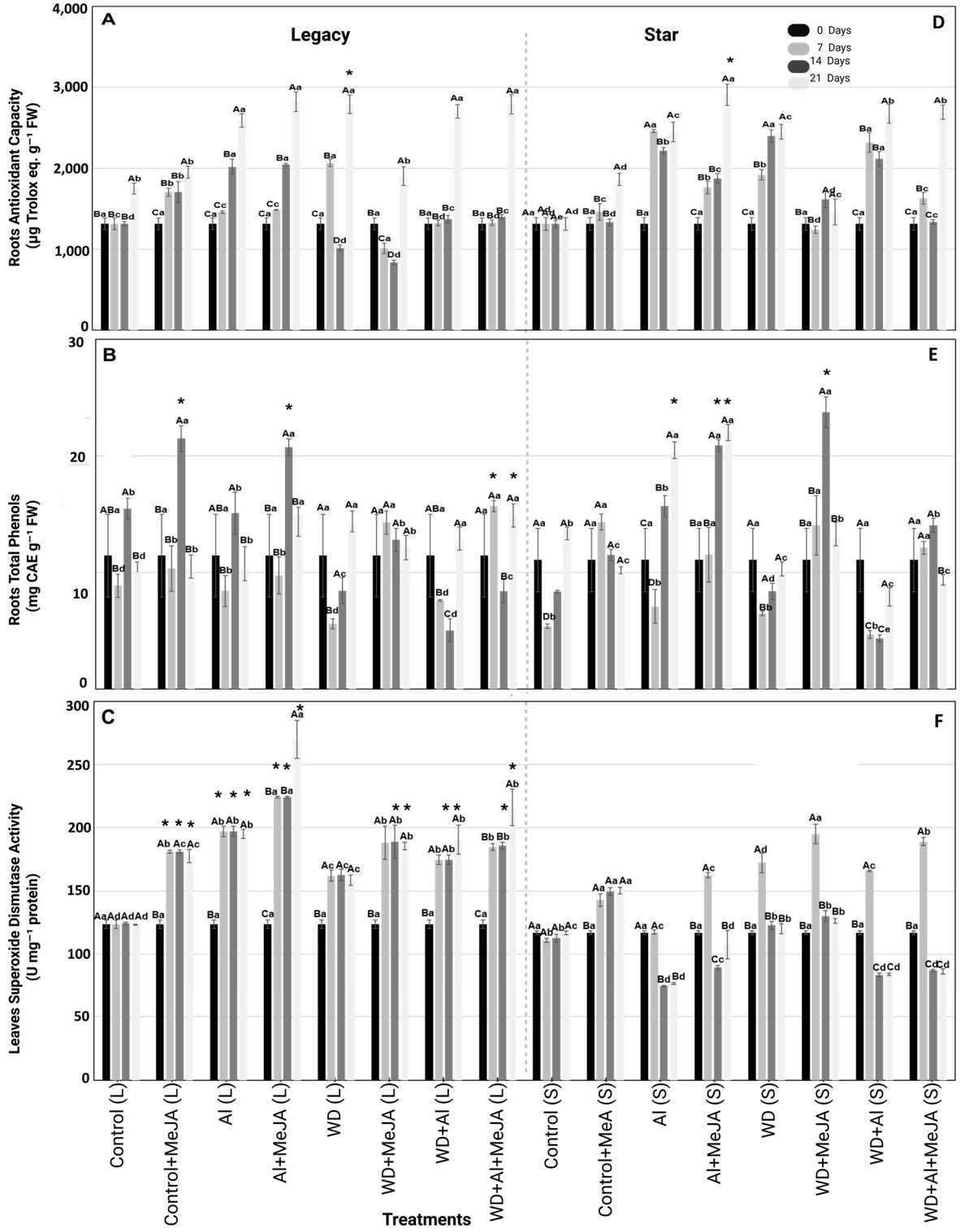


**Figure 10.** Antioxidant response of *V. corymbosum* L. cultivars Legacy and Star, under combined stress (Al + WD) and application of MeJA. (**A**,**D**) Antioxidant Activity, (**B**,**E**) Total Phenols, (**C**,**F**) SOD activity. Treatments included: Control, Aluminum (Al), WD, and combinations with MeJA (Control + MeJA, Al + MeJA, WD + MeJA, Al + WD + MeJA). Different capital letters indicate significant differences among times within each cultivar and treatment (ANOVA, Tukey HSD, $p < 0.05$). Different lower case letters indicate significant differences among treatments within each cultivar and time (ANOVA, Tukey HSD, $p < 0.05$). Asterisks (*) indicate significant differences between cultivars for the same treatment and time.

In leaves, antioxidant activity ranged from 3500 to 10,000 µg Trolox $g^{-1}$ FW, showing strong variation depending on stress conditions, exposure time, and MeJA application (Figure 9A). Under control conditions, both cultivars showed similar values with no significant differences, indicating comparable constitutive antioxidant capacity. However, under stress conditions, large differences were observed (Figure 9A). Aluminum treatment produced moderate increases of 20–35% in Legacy. WD induced the strongest response, with increases of 60–100%, while combined stress (Al + WD) produced intermediate increases of 50–70% relative to the control. The application of MeJA further enhanced antioxidant activity in both cultivars. In Al + MeJA, values increased by 25–40% compared with Al (Figure 9A). Under WD + MeJA, increases ranged from 40 to 70% relative to WD, and in Al + WD + MeJA, increases reached 45–80% compared with Al + WD, corresponding to the highest values recorded in the study. Between cultivars, Star generally showed higher antioxidant activity than Legacy, with differences of 15–30%, particularly under WD and WD + MeJA and most clearly at 21 days (Figure 9A).

Total phenols showed trends similar to those observed for antioxidant activity, with concentrations in leaves approximately three times higher than in roots (Figures 9B and 10B). Maximum phenolic accumulation was observed in treatments with MeJA (WD + MeJA and Al + WD + MeJA), although the peak occurred at 14 days rather than 21 days. In leaves, total phenol concentrations ranged from 10 to 80 mg CAE $g^{-1}$ FW, indicating strong variation depending on stress conditions and MeJA application (Figure 9B). Under $Al^{3+}$ stress, moderate increases were observed in both cultivars, reaching 20–35% in Legacy and 40–65% in Star relative to the control. WD produced the strongest phenolic response, with increases of 70–110% in Legacy and 90–130% in Star (Figure 9B). Combined stress (Al + WD) also induced substantial increases, ranging from 60 to 100% compared with the control. Exogenous MeJA application enhanced phenolic accumulation in all stress treatments. In Al + MeJA, phenol levels increased by 20–30% compared with Al alone. The WD + MeJA treatment produced the highest values observed in the study, reaching increases of 120–185% relative to the control. In Al + WD + MeJA, intermediate values were recorded, indicating partial recovery under combined stress. Across treatments, the Star cultivar accumulated on average 20–40% more total phenols than Legacy, particularly under WD and combined stress conditions (Figure 9B).

To evaluate the activation of the enzymatic antioxidant system, SOD activity was quantified. This activity in leaves and roots showed statistically significant differences among treatments, sampling times, cultivars, and their interactions ($p < 0.001$) (Figures 9C and 10C). A clear spatial pattern was observed, with SOD activity approximately 1.5 times higher in leaves than in roots (Figures 9C and 10C). A temporal pattern was also detected, with maximum enzyme activity recorded at 21 days. In leaves, SOD activity ranged from 120 to 360 U $mg^{-1}$ protein, with variations depending on stress conditions, exposure time, and MeJA application (Figure 9C). Under control conditions, both cultivars showed similar baseline SOD levels (approximately 150 U $mg^{-1}$ protein), indicating a stable redox balance. Under $Al^{3+}$ stress, SOD activity increased moderately, reaching values up to 40% higher than the control. WD induced a stronger increase, ranging from 60 to 80%, whereas combined stress (Al + WD) produced the most pronounced response, with increases of 100–120% above control values, particularly in the Legacy cultivar (Figure 9C). The exogenous application of MeJA further enhanced SOD activity under all stress treatments. In Al + MeJA, enzyme activity increased by 35–50% compared with Al alone. Under WD + MeJA, increases of 70–80% were observed, while in Al + WD + MeJA, SOD activity reached the highest values recorded in the experiment, approximately 120% above control levels. Regarding cultivar differences, Legacy consistently showed higher

SOD activity than Star, with values approximately 20–30% greater across treatments. In contrast, Star exhibited larger temporal fluctuations in enzyme activity (Figure 9C).

At the root level, antioxidant activity ranged from 1000 to 3000 μg Trolox $g^{-1}$ FW, consistently lower than that observed in leaves (Figure 10A). Under $Al^{3+}$ stress, antioxidant activity increased moderately, with values 20–30% higher than the control. WD induced a stronger response, with increases of 40–70%, whereas combined stress produced a more variable response, with the highest values recorded at 21 days, ranging from 25 to 90% above control levels (Figure 10A). The MeJA application further stimulated antioxidant activity under all stress conditions. In Al + MeJA, increases of 25–40% were observed compared with Al alone. Under WD + MeJA, the response was more pronounced, reaching increases of 50–70% relative to WD. In Al + WD + MeJA, antioxidant activity increased by 20–40% compared with Al + WD. Across treatments, the Star cultivar consistently showed higher antioxidant activity than Legacy, with differences of approximately 20–25%, particularly under WD and WD + MeJA, indicating a stronger activation of the non-enzymatic antioxidant system in this cultivar (Figure 10A).

In roots, total phenols ranged from 4 to 28 mg CAE $g^{-1}$ FW (Figure 10B). Under control conditions, both cultivars showed some variability across sampling times but remained within similar baseline ranges. The stress treatments followed patterns similar to those observed in leaves. Under $Al^{3+}$ stress, phenolic levels increased moderately by 25–40% compared with the control. WD induced a stronger response, with increases of 60–80%. In contrast, combined stress (Al + WD) resulted in intermediate increases of around 50% relative to control plants (Figure 10B). The exogenous application of MeJA significantly stimulated phenolic accumulation in roots under all stress conditions. The pattern of response was similar to that observed in leaves, with increases following the order WD + MeJA > Al + WD + MeJA > Al + MeJA. Differences between cultivars were less pronounced than those observed in leaves, but Star showed slightly higher values than Legacy (10–20%), particularly under WD and WD + MeJA (Figure 10B).

Superoxide dismutase activity in roots showed significant differences among treatments, cultivars, sampling times, and their interaction ($p < 0.001$) (Figure 10C). Values ranged from 90 to 310 U $mg^{-1}$ protein and were consistently lower than those observed in leaves. Under $Al^{3+}$ stress, SOD activity increased by 30–40% compared with the control. WD produced a stronger response, with increases of 60–75%, while combined stress (Al + WD) resulted in the highest SOD activity observed in the absence of MeJA, reaching increases of up to 100% relative to the control (Figure 10C). As observed in leaves, the exogenous application of MeJA further stimulated SOD activity under all stress conditions. In Al + MeJA, SOD activity increased by 25–30% compared with Al alone. Under WD + MeJA, increases of 40–50% were detected relative to WD, while in Al + WD + MeJA, the highest SOD values in roots were observed, reaching increases of up to 120% compared with the control. Regarding cultivar differences, the general pattern was similar to that observed in leaves. Legacy consistently exhibited higher SOD activity than Star, with differences of approximately 20–25% and a more stable response over time (Figure 10C).

### *3.5. Principal Component Analysis (PCA) and Correlation*

Multivariate principal component analysis (PCA) and correlation analyses were performed considering the three experimental time points (7, 14, and 21 days), the two cultivars (Legacy and Star), and the two analyzed tissues (leaves and roots). For the PCA, all physiological and biochemical variables measured in each tissue were included and analyzed separately. Correlation analyses focused mainly on the relationships among the main stress treatments (Al, WD, and Al + WD) and on differences between tissues.

In the PCA of leaf variables, the first two principal components (PC1 and PC2) consistently explained more than 50% of the total variance, although the cumulative variance never exceeded 60%. This distribution reflects the relatively high number of variables included in the analysis (more than 25), which tends to distribute the explained variance across multiple components. However, when the first four components (PC1–PC4) were considered together, the cumulative explained variance exceeded 70% (Figure 11).

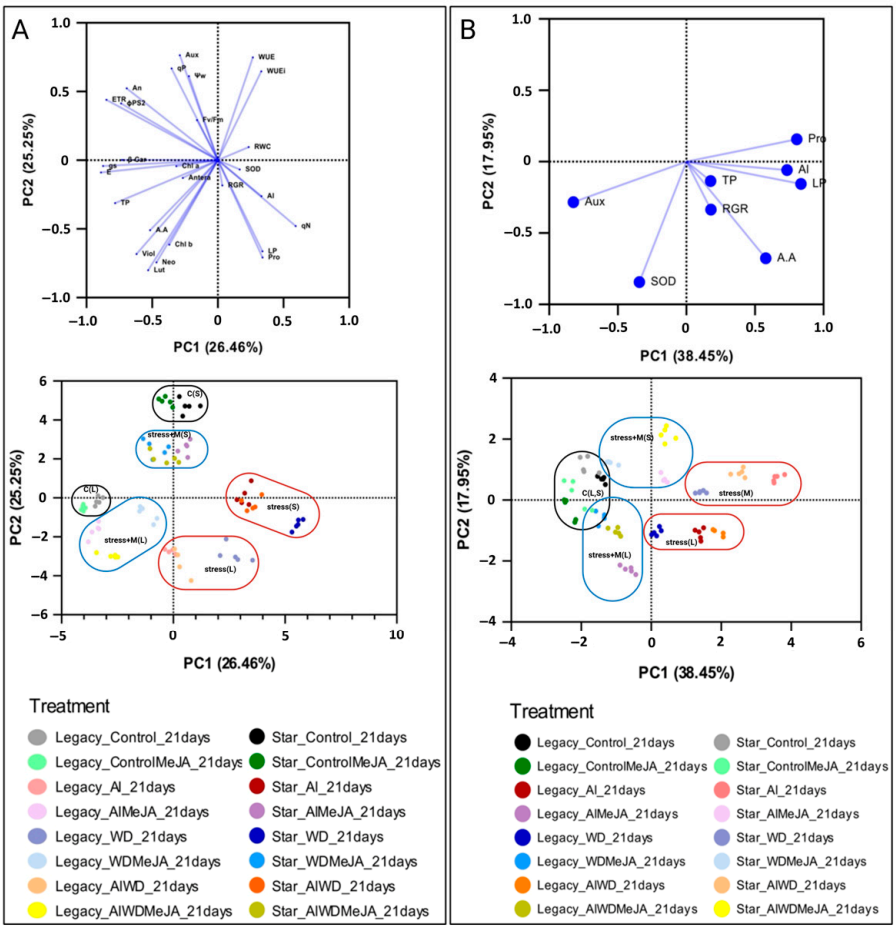


**Figure 11.** Principal Component Analysis (PCA) of physiological and biochemical parameters in leaves (**A**) and roots (**B**) of *V. corymbosum* cultivars Legacy and Star after 21 days of treatment. PCA scores plot showing the distribution and separation of treatments for both cultivars under control, aluminum (Al), WD, and combined Al + WD stresses, with or without MeJA application. Variables included in the analysis were: aluminum accumulation (Al), auxins (Aux), leaf water potential (Ψw), relative water content (RWC), proline content (Pro), net photosynthetic rate (An), stomatal conductance (gs), E, effective quantum yield of Photosystem II (ΦPSII), maximum quantum efficiency of Photosystem II (Fv/Fm), photochemical quenching (qP), non-photochemical quenching (qN), electron transport rate (ETR), water use efficiency (WUE), intrinsic water use efficiency (WUEi), chlorophyll a (Chl a), chlorophyll b (Chl b), lutein (Lut), neoxanthin (Neo), violaxanthin (Viol), antheraxanthin (Antera), lipid peroxidation (LP), antioxidant activity (A.A.), total phenols (TP), and superoxide dismutase activity (SOD).

The variables with the greatest contribution to the first principal component (PC1) were Al (Al accumulation), An, LP (lipid peroxidation), and proline, which showed the highest negative correlations. The second component (PC2) was mainly associated with auxins, water use efficiency (WUE), and chlorophyll-related variables, with a smaller contribution from xanthophyll pigments.

This multivariate structure indicates that variables related to oxidative stress (LP, Pro, and Al) and photosynthetic performance (An, ETR, and ΦPSII) are primarily responsible for distinguishing responses between treatments. Although the relationships among variables varied slightly across sampling times, the general patterns of association were maintained.

As the greatest physiological and biochemical differences were observed at 21 days in most parameters, this time point was used as a representative model for PCA interpretation (Figure 11A). Strong associations were observed among LP, Pro, Al, and qN, indicating a close relationship between oxidative stress, osmoprotectant accumulation, and non-photochemical energy dissipation. Photosynthetic variables such as An, ETR, ΦPSII, Fv/Fm, and qP were also strongly correlated with each other, forming a cluster associated with photosynthetic performance.

Additional associations were observed between water-status variables (Ψw, gs, and E) and photosynthetic pigments, suggesting coordinated responses between stomatal regulation and the photosynthetic apparatus under stress conditions. In contrast, variables such as RGR, RWC, SOD, and Fv/Fm were located closer to the center of the biplot, indicating lower contributions to overall variability and a more stable behavior across treatments. In contrast, the most dynamic variables positioned farther from the origin, including Al, LP, Pro, E, gs, and several photosynthetic parameters (An, ETR, ΦPSII), showed greater variance and stronger discriminatory power among treatments (Figure 11A).

Overall, the PCA revealed a clear separation between cultivars, with no overlap between Legacy and Star, confirming significant differences in their overall physiological and biochemical responses ($p < 0.001$) (Figure 11A). In Legacy, the Control and Control + MeJA treatments were grouped in the negative quadrant of PC1, associated with high photosynthetic performance (An, ΦPSII, ETR), low lipid peroxidation (LP), and stable pigment-related variables. The treatments exposed to Al, WD, and Al + WD progressively shifted toward positive PC1 values, mainly in the central and lower-right sectors of the biplot, indicating increased oxidative stress–related variables and reduced photochemical efficiency. In contrast, the Star cultivar showed a different distribution pattern. Control and Control + MeJA treatments clustered in a compact group in the upper central region of the plot, whereas stress treatments were more widely dispersed along both PC1 and PC2 axes. The positive quadrant of PC1 was mainly associated with higher lipid peroxidation (LP), Al accumulation (Al), and proline content, together with reduced photosynthetic efficiency (An, ΦPSII, ETR). In all cases, treatments including MeJA under stress conditions (Al + MeJA, WD + MeJA, and Al + WD + MeJA) were positioned closer to the control treatments, indicating a shift toward the physiological state observed under non-stress conditions (Figure 11A).

In roots, the PCA at 21 days revealed a more heterogeneous multivariate pattern than that observed in leaves (Figure 11B). Root responses also showed greater temporal variability. At 7 days, strong linear correlations were observed, suggesting an acute stress response. At 14 days, the analysis showed higher dispersion and variability, suggesting a phase of metabolic reconfiguration. By 21 days, the multivariate patterns in roots tended to stabilize and more closely resemble those observed in leaves, indicating partial recovery of physiological balance. A positive association among Pro, LP, and Al was maintained, with these variables located in the right quadrant of PC1, indicating their coordinated response under severe stress conditions. In contrast, SOD showed an inverse relationship with these variables, consistent with its role in the antioxidant response.

Complementary analyses at the final sampling time (21 days) also revealed additional relationships. A positive association among relative growth rate (RGR), total antioxidant activity (A.A.), and total phenols (TP) was observed, especially in the Star cultivar, suggesting the activation of antioxidant mechanisms. Additionally, a relationship between SOD

and auxins (Aux) was identified in Legacy (Figure 11B), suggesting a potential coordination between enzymatic antioxidant responses and auxin concentration under stress conditions.

PC1 was mainly defined by lipid peroxidation (LP), Al accumulation, and proline (Pro) content. Superoxide dismutase activity showed a strong negative loading on PC2, indicating that this enzyme accounted for a large portion of the variability associated with antioxidant responses among cultivars and treatments. The clustering pattern revealed a clear separation between treatments with and without MeJA application. Stress treatments without MeJA were mainly located in the positive quadrant of PC1 and were associated with higher LP, Pro, and Al values. This pattern was particularly evident in the Star cultivar, which showed greater point dispersion and higher intragroup variability, suggesting a less stable metabolic response under combined stress conditions (Figure 11B).

In contrast, Legacy displayed a more compact clustering pattern and lower variability, indicating greater physiological stability and adaptive capacity under multiple stress conditions. Treatments including MeJA (Al + MeJA, WD + MeJA, and Al + WD + MeJA) were positioned closer to the control treatments, indicating a shift toward the physiological state observed under non-stress conditions (Figure 11B). This pattern was consistent with the distribution observed in leaf tissues.

The heatmap shows the multivariate correlation patterns among physiological, biochemical, and antioxidant variables. The correlation heatmap revealed statistically significant differences between the Legacy and Star cultivars, indicating distinct physiological responses to the same stress factors.

In the Legacy cultivar, the heatmap revealed a highly cohesive photosynthetic cluster characterized by strong positive correlations (r = 0.66–0.85) among ΦPSII, ETR, qP, and Fv/Fm, as well as consistent associations with An, gs, E, and WUEi. These variables formed a distinct module in the dendrogram, indicating low statistical distance and strong functional integration among photosynthetic parameters. A second group of associations corresponded to a low-intensity oxidative stress composed of LP, qN, Al concentration, and proline. This association showed moderate correlations ($r < 0.55$) and appeared as a separate cluster from the photosynthetic parameters, with greater Euclidean distance in the dendrogram. The weak correlation between SOD and LP ($r < 0.30$) suggests that oxidative stress did not reach levels sufficient to activate this enzyme in this cultivar. Photosynthetic pigments (Chl a, Chl b, lutein, neoxanthin, violaxanthin, and β-carotene) formed another group of positive correlations (r = 0.33–0.66). This pigment cluster tended to associate with the photosynthetic parameters and showed moderate negative correlations with LP and Al.

Antioxidant variables showed contrasting patterns between cultivars. In Star, SOD was positively correlated with LP ($r > 0.50$), suggesting a stronger antioxidant response to oxidative stress. In contrast, total antioxidant activity (AA) showed negative correlations with photosynthetic parameters and pigments and occupied more peripheral positions in the dendrogram, suggesting a lower contribution to the stabilization of the photosynthetic system (Figure 12A).

The heatmap analysis of root variables in the Legacy cultivar revealed a simple, stable, and functionally integrated association (Figure 12C). A dominant module associated with growth, auxins, and antioxidants was identified, in which relative growth rate (RGR), auxin concentration (Aux), and total phenols (CAE) were grouped with strong positive correlations ($r > 0.70$). This pattern suggests the maintenance of root growth and preservation of auxin levels under the evaluated conditions. The relationship associated with oxidative stress was defined by lipid peroxidation (LP), proline (Pro), and superoxide dismutase activity (SOD), which showed moderate positive correlations among these variables. However, this relation showed no strong association with Al accumulation, suggesting that oxidative stress remained contained. The coordinated presence of Pro and SOD within this

cluster indicates the activation of osmotic and enzymatic antioxidant responses without evidence of severe metabolic disruption. (Figure 12C).

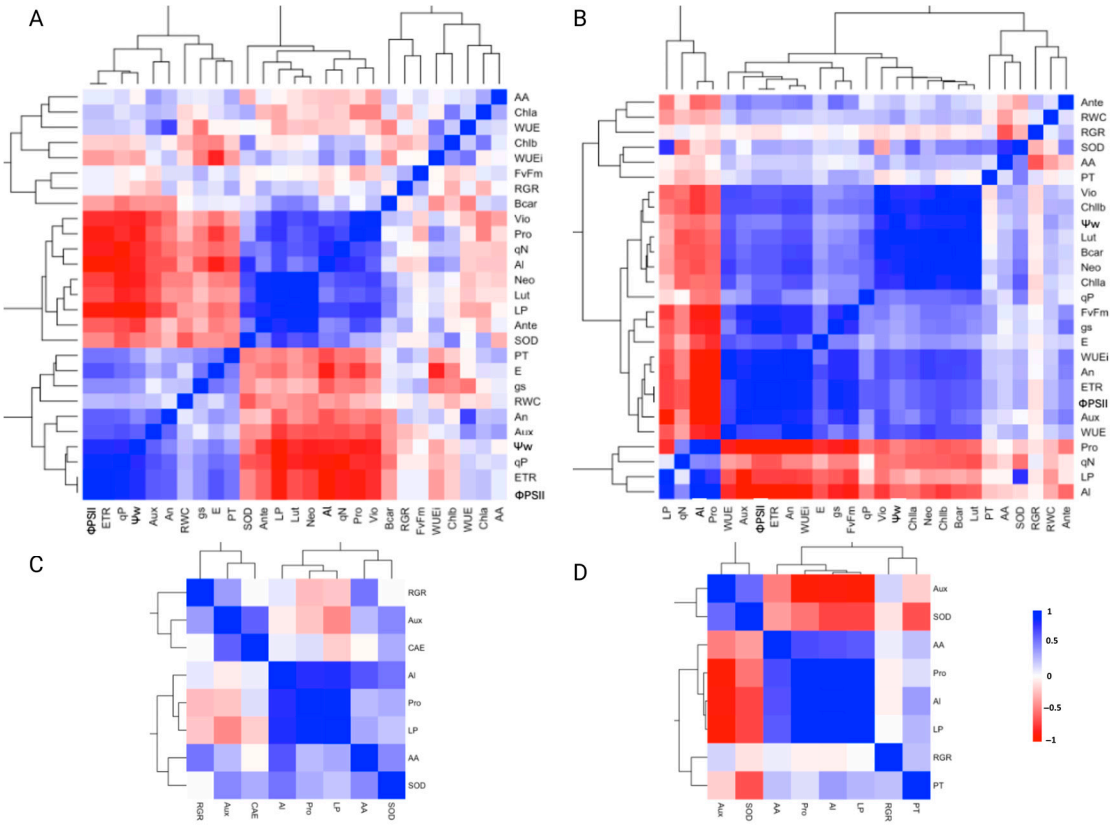


**Figure 12.** Heatmap of physiological and biochemical parameters in leaves ((**A**) (Legacy), (**B**) (Star)) and roots (**C**) (Legacy), (**D**) (Star)) of *V. corymbosum* cultivars under aluminum (Al). Variables included in the analysis were: aluminum accumulation (Al), auxins (Aux), leaf water potential (Ψw), relative water content (RWC), proline content (Pro), net photosynthetic rate (An), stomatal conductance (gs), E, effective quantum yield of Photosystem II (ΦPSII), maximum quantum efficiency of Photosystem II (Fv/Fm), photochemical quenching (qP), non-photochemical quenching (qN), electron transport rate (ETR), water use efficiency (WUE), intrinsic water use efficiency (WUEi), chlorophyll a (Chl a), chlorophyll b (Chl b), lutein (Lut), neoxanthin (Neo), violaxanthin (Viol), antheraxanthin (Antera), lipid peroxidation (LP), antioxidant activity (A.A.), total phenols (TP), and superoxide dismutase activity (SOD).

In contrast, the Star cultivar showed an opposite correlation pattern. The heatmap revealed a dominant oxidative stress composed of LP, Pro, qN, and Al, which showed very strong positive correlations ($r = 0.66–0.90$). These variables formed a compact cluster in the dendrogram, indicating strong co-variation and low statistical distance among stress-related parameters. The photosynthetic parameters in Star, including ΦPSII, qP, Fv/Fm, ETR, An, gs, E, and WUE, remained internally cohesive ($r > 0.60$). However, this group showed strong negative correlations with the oxidative damage parameters ($r < -0.66$), indicating an inverse relationship between oxidative damage and photosynthetic performance. The pigment module in Star showed moderate to strong negative correlations with LP and Al ($-0.33 < r < -0.66$), suggesting a stress-associated decline in pigment stability. Unlike in Legacy, pigment variables were not fully integrated into the main photosynthetic module. They appeared as an intermediate cluster in the dendrogram, indicating weaker co-regulation with photosynthetic parameters.

Overall, the hierarchical structure in Star revealed two clearly differentiated modules, one associated with Al-induced damage and another associated with photosynthetic

integrity. In contrast, Legacy exhibited a more integrated structure, characterized by a dominant photosynthetic module and lower influence of the stress-associated cluster (Figure 12B).

Star roots showed similar modules, but the oxidative module had a stronger impact, with stress clearly dominating growth-related functions. Al, LP, Pro, and SOD showed very strong correlations ($r > 0.80$), reflecting high accumulation of Al in root tissues, severe oxidative damage (LP), activation of SOD as a response to high ROS production, and an exacerbated osmotic response (Pro).

Total antioxidant activity (AA) showed strong negative correlations with LP and Al, indicating depletion of non-enzymatic antioxidants. A second functional module composed of RGR, Aux, and CAE formed a small cluster that was negatively correlated with the damage module. This pattern was associated with suppression of root growth, strong auxin inhibition, suggesting involvement of the apical meristem, and reduced CAE (Figure 12D).

The multivariate pattern of Legacy under WD showed a dominant set of photosynthetic parameters characterized by high-magnitude positive correlations ($r = 0.65–0.90$) among ΦPSII, qP, ETR, Fv/Fm, An, gs, E, and the water-use efficiencies WUE and WUEi. This cluster showed a low Euclidean distance in the dendrogram.

The integration of RWC within this module reinforces the idea that Legacy maintains a moderate water status, although it remains subject to stomatal closure. Positive correlations between WUE and WUEi, and between photochemical efficiency parameters, suggest that a plant regulates stomatal opening without compromising PSII functionality. From a statistical perspective, this module explains most of the shared variance in Legacy, confirming that photosynthetic performance represents the dominant axis under WD. The oxidative stress module in Legacy was small and showed low cohesion, with correlations ranging from $r = 0.30$ to 0.55 among LP, Pro, qN, and SOD. LP showed moderate negative correlations with the photosynthetic module (r ca. $-0.35$).

Total antioxidant activity (AA) showed low correlations with damage variables and appeared closer to the pigment module, suggesting a preventive antioxidant role. Photosynthetic pigments formed a stable cluster with moderate positive associations with ΦPSII and ETR ($r = 0.40–0.70$) and weak negative correlations with LP. The pigment structure remained intact, indicating stability of the photosynthetic apparatus even under water stress. Overall, the Legacy dendrogram revealed two well-defined modules. A dominant photosynthetic module that was highly cohesive and functional, and a smaller secondary stress module with lower statistical influence (Figure 13A).

In roots, the Legacy pattern showed structural and functional stability even under WD. A dominant and cohesive growth–auxin–antioxidant module was identified, in which RGR, Aux, and PT were grouped in a block with strong positive correlations ($r > 0.70$). A second module corresponded to a mild oxidative response and included LP, Pro, and SOD, showing moderate positive correlations. Total antioxidant activity (AA) was positioned between both modules, suggesting a balance between protective antioxidant responses and stress-related signals (Figure 13C).

The Star heatmap showed a completely different pattern from that of Legacy. The oxidative stress module was the largest and most intense in the matrix, encompassing LP, Pro, qN, SOD, and Ψw. These variables showed very strong positive correlations ($r = 0.75–0.95$). The dendrogram revealed an extremely compact cluster, indicating that the oxidative response statistically dominated leaf behavior in this cultivar under WD.

LP correlated positively with qN, Pro, and SOD and negatively with all photosynthetic variables ($r < -0.70$). Ψw showed very strong negative associations with functional parameters, indicating a marked loss of leaf hydration. Statistically, this module explained a large portion of the total variance in the Star matrix, indicating a predominant stress

response. The photosynthetic module, composed of ΦPSII, qP, ETR, Fv/Fm, An, gs, E, and WUE, remained internally cohesive (r = 0.60–0.85) but showed strong negative correlations (r < −0.70). This pattern reflects reductions in ΦPSII and Fv/Fm, indicating impairment of PSII, accompanied by a marked decrease in ETR.

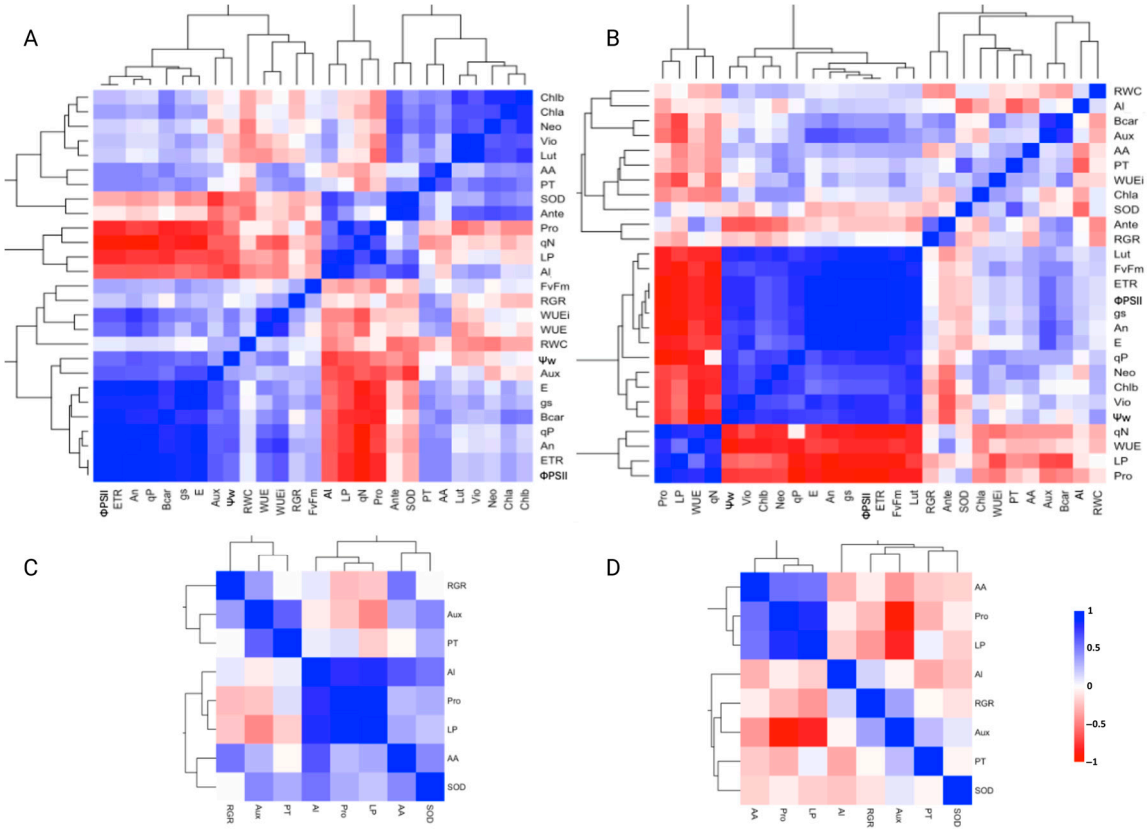


**Figure 13.** Heatmap of physiological and biochemical parameters in leaves ((**A**) (Legacy), (**B**) (Star)) and roots ((**C**) (Legacy), (**D**) (Star)) of *V. corymbosum* cultivars under DW. Variables included in the analysis were: aluminum accumulation (Al), auxins (Aux), leaf water potential (Ψw), relative water content (RWC), proline content (Pro), net photosynthetic rate (An), stomatal conductance (gs), E, effective quantum yield of Photosystem II (ΦPSII), maximum quantum efficiency of Photosystem II (Fv/Fm), photochemical quenching (qP), non-photochemical quenching (qN), electron transport rate (ETR), water use efficiency (WUE), intrinsic water use efficiency (WUEi), chlorophyll a (Chl a), chlorophyll b (Chl b), lutein (Lut), neoxanthin (Neo), violaxanthin (Viol), antheraxanthin (Antera), lipid peroxidation (LP), antioxidant activity (A.A.), total phenols (TP), and superoxide dismutase activity (SOD).

Simultaneously, gs and E decreased abruptly, indicating strong stomatal closure. The pigment module showed scattered correlations and strong negative associations with LP and qN, suggesting degradation of the xanthophyll pool. This pigment disorganization was reflected in inconsistent correlations between carotenoids and photosynthetic parameters, a pattern typically associated with photooxidative stress. Auxins and total proteins appeared in marginal positions in the dendrogram, showing moderate negative correlations with LP and Pro (r ca. −0.40) (Figure 13B).

Star roots showed an architecture dominated by stress, which was even more pronounced than in leaves. An oxidative damage module dominated by Pro, LP, Al, and SOD showed very strong correlations among these variables (r > 0.80). The marked increase in LP and the high proline levels suggest stress damage under severe stress. A second module corresponded to the functional group composed of RGR, Aux, and PT. These variables showed negative correlations with the oxidative parameters. This pattern indicates

strong inhibition of root growth associated with a severe reduction in auxin levels and a decline in PT. The dendrogram revealed clear dominance of the stress module across the matrix, indicating extreme susceptibility of Star roots under the evaluated stress conditions (Figure 13D).

Analysis of the heatmap for Legacy leaves subjected to combined Al and WD stress (Al–WD) revealed a highly organized multivariate structure dominated by a robust photosynthetic–hydraulic module and a smaller oxidative stress module. Overall, the correlation matrix indicates that even under simultaneous conditions of Al toxicity and dehydration, Legacy maintains stable physiological parameters and avoids the stress damage observed in more sensitive cultivars. Variables associated with photochemical performance and gas exchange, including ΦPSII, qP, ETR, Fv/Fm, An, gs, and E, together with indicators of water use efficiency (WUE and WUEi) and leaf water status (Ψw and RWC), formed a block of strong positive correlations ($r > 0.70$) represented by a cohesive cluster in the dendrogram. This statistical pattern reflects close co-regulation between PSII quantum yield, electron transport rate, and stomatal opening. Water-use efficiency remained strongly integrated with PSII functioning, as indicated by the positive associations between WUE and WUEi and photochemical variables. Positive correlations between RWC, Ψw, and the photosynthetic module further suggest the capacity to maintain water status under combined stress conditions.

A second cluster included LP, Pro, qN, SOD, and Al and showed moderate positive correlations ($r = 0.40–0.65$). This module did not displace the photosynthetic module, suggesting that although oxidative stress was present, it remained controlled. The statistical structure of this module included a consistent association among LP, Pro, and qN, moderate correlations between LP and Al, and intermediate activation of antioxidant responses represented by SOD.

Pigment variables formed an additional stability module that remained positively associated with the photosynthetic cluster. Chlorophylls (Chla and Chlb) and most carotenoids (Lut, Neo, Vio, Bcar, and Ante) showed moderate positive correlations with ΦPSII, Fv/Fm, and ETR ($r = 0.40–0.75$), indicating maintenance of pigment–photochemistry integration under combined stress. Antioxidant activity (AA) was also statistically associated with the photosynthetic parameters and with pigment variables. SOD showed moderate correlations with LP and Pro but did not reach values indicative of a critical oxidative response, suggesting effective control of redox balance in Legacy leaves under combined stress conditions (Figure 14A).

In Legacy roots, the multivariate pattern was qualitatively and quantitatively distinct. The heatmap revealed a dominant functional module comprising RGR, Aux, PT, and, to a lesser extent AA, with strong positive correlations (r ca. 0.65–0.90) among these variables. This cluster showed low Euclidean distance in the dendrogram and dominated the overall architecture, indicating that root growth, primary metabolism, and auxin concentration remained operational under combined stress conditions. No strong negative correlations were detected between this module and the stress variables, indicating the absence of severe growth inhibition. The oxidative stress module, including LP, Pro, SOD, Al, and partially AA, was smaller and moderately cohesive. LP and Pro showed positive correlations, but did not reach extreme intensities. SOD showed intermediate correlations with LP and Pro, consistent with efficient but not excessive antioxidant activation. Aluminum accumulation showed a moderate association with LP, indicating that the metal contributed to oxidative damage but did not dominate the matrix structure. Total antioxidant activity (AA) showed a mixed correlation pattern, without evidence of depletion, which is consistent with a tolerance response in Legacy roots under combined stress (Figure 14C).

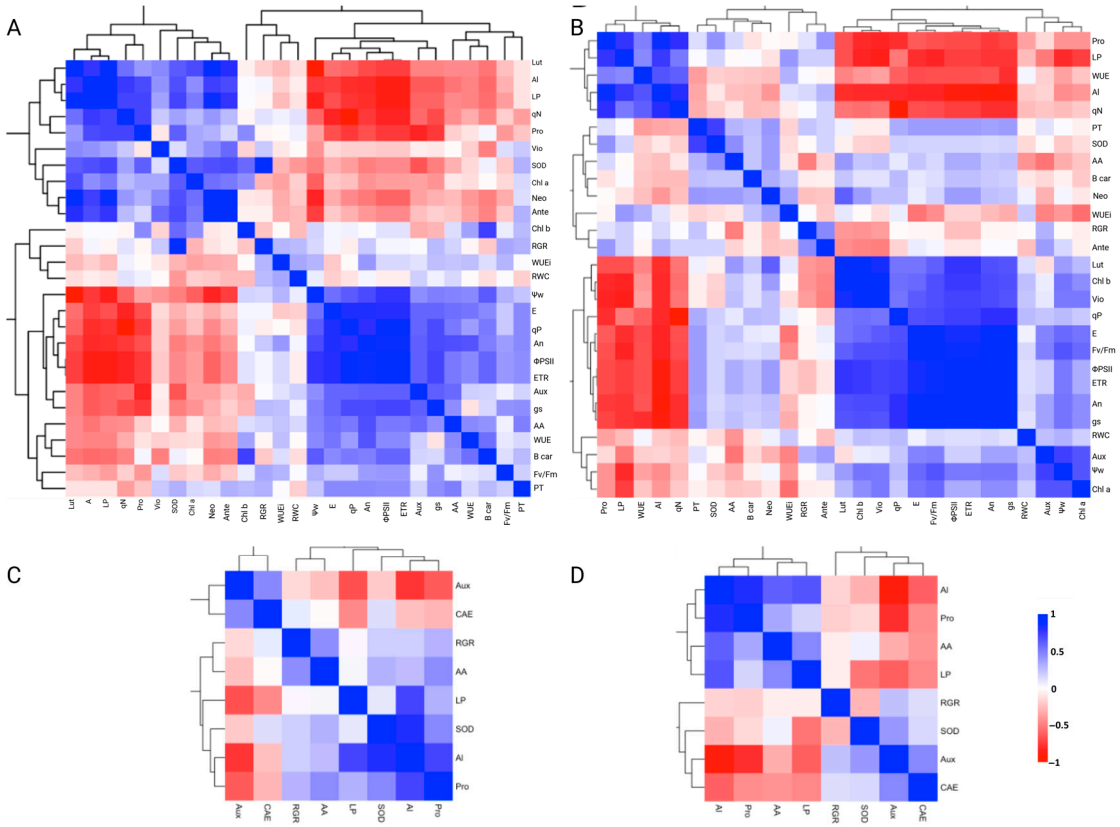


**Figure 14.** Heatmap of physiological and biochemical parameters in leaves ((**A**) (Legacy), (**B**) (Star)) and roots ((**C**) (Legacy), (**D**) (Star)) of *V. corymbosum* cultivars under DW and Aluminum (Al). Variables included in the analysis were: aluminum accumulation (Al), auxins (Aux), leaf water potential (Ψw), relative water content (RWC), proline content (Pro), net photosynthetic rate (An), stomatal conductance (gs), E, effective quantum yield of Photosystem II (ΦPSII), maximum quantum efficiency of Photosystem II (Fv/Fm), photochemical quenching (qP), non-photochemical quenching (qN), electron transport rate (ETR), water use efficiency (WUE), intrinsic water use efficiency (WUEi), chlorophyll a (Chl a), chlorophyll b (Chl b), lutein (Lut), neoxanthin (Neo), violaxanthin (Viol), antheraxanthin (Antera), lipid peroxidation (LP), antioxidant activity (A.A.), total phenols (TP), and superoxide dismutase activity (SOD).

High-intensity oxidative stress modules dominated Star correlational architecture, whereas in Legacy, a dominant functional module, either photosynthetic or growth-related, remained active, and stress variables were statistically less influential. In Star leaves, the heatmap showed the most severe and disorganized pattern among all treatments evaluated for this cultivar. The matrix was structured into two strongly contrasting blocks. One corresponded to an oxidative damage module and the other to a decreased photosynthetic module that was strongly repressed and negatively correlated with the damage module. The oxidative damage module included LP, Pro, Al, qN, SOD, PT, and AA. LP behaved as a central variable and showed very strong positive correlations ($r > 0.80$) with Pro, SOD, and Al, indicating a critical peak of oxidative damage associated with the combination of WD and Al toxicity. The qN was positively associated with LP, indicating increased non-photochemical energy dissipation. Antioxidant activity (AA) showed very low or negative correlations with this module, indicating a decrease in the non-enzymatic antioxidant system. Together, these variables formed the statistically dominant cluster and explained the largest proportion of shared variance in the matrix. The photosynthetic module grouped variables such as Fv/Fm, ΦPSII, qP, ETR, An, gs, E, WUE, WUEi, RWC and Ψw. Within this module, correlations remained moderate to high and positive. However, the module showed very strong negative correlations ($r < -0.70$) with LP, Pro, and Al. This pattern

indicates a strong photochemical decrease, as reflected in Fv/Fm, ΦPSII, and ETR, and in simultaneous reductions in gs and An, with pronounced stomatal closure and severe $CO_2$ diffusive limitation. Negative correlations with RWC and Ψw also indicate substantial loss of leaf water status (Figure 14B).

In Star roots, the combined stress heatmap showed the most severe pattern among all root treatments. The matrix was organized around a massive oxidative stress module composed of Al, LP, Pro, SOD, and AA in a depressed state. Very strong positive correlations were observed among Al, LP, and Pro, as well as strong associations with SOD. In contrast, AA showed negative or low-magnitude correlations with this module, indicating depletion of the non-enzymatic antioxidant system. At the same time, the growth module composed of RGR, Aux, and CAE appeared to be strongly suppressed. RGR showed strong negative correlations with LP and Al. Aux showed negative correlations with Al, LP, and Pro. The dendrogram separated a highly cohesive, dominant stress module composed of Al, LP, Pro, and SOD from a small, weak functional module composed of RGR, Aux, and CAE. This functional module appeared isolated and strongly reduced, indicating that stress conditions largely governed root physiology in Star under combined $Al^{3+}$ toxicity and WD (Figure 14D).

## 4. Discussion

Climate change has intensified multiple constraints on agricultural systems, increasing the frequency and severity of abiotic stresses such as WD and $Al^{3+}$ phytotoxicity. These constraints are particularly pronounced in acidic volcanic soils, including Andisols, which are characterized by low pH and limited water availability [1–3]. Considering this context, the present study evaluated the individual and combined effects of Al toxicity and WD on *V. corymbosum*, as well as the potential of MeJA to modulate stress-response mechanisms. The results showed that both cultivars exhibited marked impairments in vegetative growth, plant water status, and photosynthetic performance under individual stress conditions, with particularly pronounced effects observed under combined Al and WD stress (Al + WD).

### *4.1. Aluminum Toxicity, Root Growth, and Auxin Concentration*

Our results indicate that the Star cultivar exhibited higher Al accumulation in leaves and roots under Al and combined stress (Al + WD) treatments (Figure 1). These differences suggest distinct mechanisms of root Al-exclusion and leaf Al compartmentalization between sensitive and tolerant cultivars [7,17,45]. The greater accumulation of Al in the roots of Star indicates a lower efficiency of Al exclusion mechanisms, resulting in increased toxicity and subsequent inhibition of root growth, as evidenced by the reduced root relative growth rate (root RGR, Figure 2B), a response typically observed in Al-sensitive genotypes [7,9].

Furthermore, root growth inhibition is widely recognized as one of the earliest symptoms of both drought and $Al^{3+}$ stress and is closely associated with reductions in auxin synthesis and transport [46–48]. In this study, exposure to individual stresses (Al or WD) significantly impaired plant growth to a degree comparable to that observed under combined stress. However, the severity of these effects was more pronounced in the sensitive cultivar (Star) than in the resistant cultivar (Legacy) (Figure 3). These contrasting responses to individual and combined stresses may be explained by differences in hormone levels, particularly auxin. Pavlović et al. [47] demonstrated that *Brassica rapa*, a drought-sensitive species, exhibited endogenous auxin levels approximately 35% lower than those of control plants, accompanied by a significant reduction in root growth. This evidence could support the interpretation that a decrease in auxin concentration reduces root growth under stress conditions, consistent with the responses observed in the present study.

Under water or $Al^{3+}$ stress, plants can increase auxin concentration, which partially supports root growth. In contrast, under combined stress, this change alone may be insufficient to maintain root growth, thus requiring the activation of additional resistance mechanisms. Therefore, the Al and Al + WD treatments resulted in a significant reduction in auxin levels, particularly in the sensitive cultivar Star (Figure 3). This decrease correlated strongly with Al accumulation (Figures 12–14) and is closely associated with the inhibition of root growth under stress conditions [46,48]. These findings indicated that $Al^{3+}$ stress directly perturbs auxin concentration, contributing to the pronounced reduction in root growth observed in the sensitive genotype Star. Previous studies have demonstrated that Al interferes with auxin transport by inhibiting polar auxin transporters, particularly PIN proteins. This effect has been documented in Arabidopsis, rice, and pea and is known to impact root elongation negatively [46,48–50]. Such inhibition could provide a possible explanation for the reduced auxin concentrations and impaired root development observed under Al and combined Al + WD treatments in Star.

On the other hand, our data show that MeJA promoted an accumulation of total auxins, particularly in the resistant cultivar Legacy, where significant increases were observed across all MeJA-treated conditions. These changes were closely associated with the increase in relative growth rate (RGR; Figure 2), supporting a functional association between auxin accumulation and plant growth under stress.

### *4.2. MeJA Promotes Osmotic Regulation as Well as Reduces Water Loss*

In blueberry plants, the imposed stress conditions directly affected plant water status, as evidenced by significant reductions in water potential (Ψw) and relative water content (RWC). Combined stress (Al + WD), WD, and, to a lesser extent, Al toxicity ($Al^{3+}$) reduced both parameters relative to the control treatments (Figure 4). Under combined Al + WD stress, the decreases in Ψw (Figure 4A) and RWC (Figure 4B) were more pronounced in the Al-sensitive cultivar Star (Figure 14), indicating greater susceptibility to osmotic and ionic imbalances compared with the tolerant cultivar Legacy. This response is consistent with observations in barley and rice, in which drought-tolerant genotypes maintain higher Ψw and RWC values. Osmotic adjustment mechanisms, including proline accumulation and increased root hydraulic conductance, contribute to this response [45,46].

Maintaining higher Ψw and RWC under stress has important implications for plant growth. Reductions in growth under stress conditions are largely attributed to WD and associated osmotic constraints, as both drought and $Al^{3+}$ stress reduce plant water potential [51]. Previous studies have identified WD as the primary driver of declines in Ψw and RWC, resulting from restricted water uptake and increased membrane permeability under osmotic stress conditions [45,52,53]. Under combined drought and $Al^{3+}$ stress, however, reductions in plant water status cannot be attributed solely to water limitation. Evidence indicates that $Al^{3+}$ further exacerbates water and nutrient constraints by directly impairing root function. Yang et al. [53] reported that under simultaneous WD and $Al^{3+}$ stress, Al predominantly reduces water and nutrient uptake by inhibiting root growth, disrupting cell division and expansion. In addition, its accumulation in the root apoplast restricts the movement of water and nutrients. The rapid binding of Al within the root apoplast can reduce cell wall porosity and limit the mobility of high-molecular-weight solutes, suggesting a direct impairment of root hydraulic conductivity. In addition, Al directly alters plasma membrane properties, including fluidity and permeability, through interactions with membrane components [7]. These membrane-level alterations collectively limit the uptake of water and essential nutrients, such as Fe, Ca, Mg, Mn, K, P, and N [12].

Under WD and combined Al + WD stress, plant water uptake is limited by reduced water availability and Al-induced root dysfunction. This constraint led to pronounced

reductions in Ψw across treatments, whereas relative water content (RWC) remained less affected, suggesting the activation of compensatory mechanisms to maintain cellular hydration. Based on our experimental data, the differential accumulation of proline among organs and cultivars was consistent with the observed RWC patterns (Figure 4B), indicating a role for proline in water retention and the stabilization of cellular structures. Plant adaptation to water stress commonly involves osmotic adjustment strategies, particularly the accumulation of compatible solutes. Osmoprotectants, including free amino acids, proline, and soluble sugars, mitigate water loss and contribute to the maintenance of cell turgor [5,23]. This mechanism has been widely reported in studies of *Pinus pinea*, *Phaseolus vulgaris*, *Triticum aestivum*, and *Zea mays*, where a strong association between proline accumulation and tolerance to water stress has been demonstrated [5,54–56].

Our experimental data show that foliar application of MeJA under combined water stress significantly reduced Al concentration (Figure 1) and increased relative growth rate (RGR), water potential (Ψw), and relative water content (RWC) compared with plants not treated with MeJA (Figures 2 and 4). The observed responses suggest that MeJA mitigates the adverse effects of combined WD and $Al^{3+}$ stress on plant water relations and performance. However, the mechanisms by which MeJA limits Al uptake under these conditions remain poorly understood. A potential mechanistic basis for the reduced Al accumulation observed in MeJA-treated plants is suggested by previous findings in highbush blueberry cultivars. Jasmonate accumulation enhances WRKY-mediated regulation of the malate transporter ALMT, promoting malate exudation into the rhizosphere and complexation of Al, thereby limiting its uptake by the plant [19].

In addition to limiting Al uptake, MeJA improves plant water status by modulating stomatal behavior. Jasmonate signaling promotes Ca transport to guard cells, facilitating stomatal closure, reducing transpiration, and attenuating declines in Ψw [57]. Water-deficit studies in *Brassica juncea* have shown that MeJA increases the accumulation of osmolytes, including proline and total soluble sugars, resulting in higher levels than those observed in untreated plants [58]. These findings support a role for MeJA in osmotic regulation under water-limited conditions.

MeJA-mediated stress tolerance extends beyond osmotic regulation and involves transcriptional and physiological reprogramming. In *Triticum aestivum*, MeJA induces the synthesis of dehydrins, a group of late embryogenesis abundant (LEA) proteins that stabilize plasma membranes and protect macromolecules from oxidative damage associated with lipid peroxidation [59]. These proteins act synergistically with antioxidant enzymes and osmoprotectants, thereby strengthening plant defense systems under WD conditions. MeJA has also been reported to modulate aquaporin expression, improving water transport efficiency and cellular hydration, thereby contributing to the maintenance of photosynthetic activity under stress [59]. Overall, these responses highlight the regulatory role of MeJA in activating stress-responsive genes and maintaining redox homeostasis, thereby contributing to enhance resilience under combined abiotic stresses [60].

### *4.3. Modulation of Photosynthetic Performance and Water-Use Efficiency*

Regarding photosynthetic and chlorophyll fluorescence parameters, plants exposed to individual stresses (Al or WD) and their combination (Al + WD) showed significant changes across all measured variables (Figure 6; Table 2). The most pronounced reductions were observed under WD, followed by combined stress (Al + WD) and, to a lesser extent, $Al^{3+}$ stress alone. No cumulative effects of combined stress were detected for An, gs, E, WUE, or WUEi (Figure 6; Table 1), nor for the maximum quantum yield of PSII (Fv/Fm) (Table 1).

Overall, most photosynthetic parameters were positively correlated with each other and negatively correlated with Al concentration and lipid peroxidation (LP) (Figures 12–14), indicating a close association between photosynthetic impairment, Al accumulation, and oxidative damage. The general effects of stress on photosynthesis observed in this study become more evident when analyzed at the cultivar level, particularly in the Al-sensitive cultivar, which exhibited a significant reduction in photosynthetic parameters.

The above-mentioned stress-induced alterations in photosynthesis have direct implications for WUE. The WUE reflects the balance between carbon assimilation and water loss under stress conditions. In this study, the cultivar Legacy exhibited significantly higher WUE values than Star across most treatments. The WD + MeJA treatment showed the highest WUE values in Legacy, whereas Star reached its maximum WUE under $Al^{3+}$ stress alone. This pattern indicates a greater capacity of Legacy to maintain WUE under stress, likely associated with more effective stomatal regulation and higher photosynthetic efficiency.

MeJA has been reported to enhance WUE by increasing net photosynthetic rate (An) and reducing transpiration (E), as observed in other species such as soybean and rapeseed [6,17]. In agreement with these observations, WUEi, calculated as the ratio between An and gs, also differed significantly among cultivars and treatments in this study. This response indicates cultivar-dependent regulation of gas exchange under stress conditions. The application of MeJA has been associated with improvements in An, gs, and E, primarily through attenuation of oxidative stress in leaf tissues. This effect has been linked to the activation of antioxidant defense systems, including SOD, catalase (CAT), and ascorbate peroxidase (APX), as well as enhanced protection of photosystem II (PSII). These responses contribute to maintaining $CO_2$ fixation and the structural integrity of the photosynthetic machinery under stress conditions [16,58,60]. MeJA can also modulate hormonal balance through interactions with ABA, SA, and auxins, thereby stabilizing stomatal function and promoting moderate stomatal opening. This regulation facilitates $CO_2$ diffusion while sustaining gs and E under stress conditions [57]. In addition, MeJA induces the accumulation of secondary metabolites, such as flavonoids and carotenoids, which protect chloroplast structures, reduce photoinhibition, and enhance photosynthetic efficiency [11,16,19,23,24].

### *4.4. Modulation of Photosynthetic Pigments and Protective Responses*

In this study, Al toxicity ($Al^{3+}$), WD, and their combined application led to significant reductions in chlorophyll content (Chl a and b) (Figure 7) and carotenoids (Table 4) in both *V. corymbosum* cultivars. These reductions were more pronounced in the Al-sensitive cultivar Star. The observed decrease in the chlorophyll a/b ratio suggests a reduction in the size of light-harvesting complexes of the photosystem II (PSII) (LHCII), which may represent an adaptive adjustment to excess excitation energy under stress conditions. However, this adjustment likely occurs at a physiological cost, as it can compromise light-harvesting capacity and, consequently, net photosynthetic efficiency.

In the Legacy cultivar, maintenance of the chlorophyll a/b ratio under stress indicates a balanced adjustment between light absorption efficiency and photoprotection, resulting in higher net photosynthetic rates compared with Star (Figure 6; Table 3). In contrast, Star exhibited a less effective adjustment, consistent with lower physiological plasticity under stress conditions. Following the MeJA application, carotenoid content increased, mainly in Legacy (Table 4). This response, combined with the increases observed in qN (Table 2), supports a role for carotenoids (including xanthophyll cycle) in photoprotection and oxidative stress mitigation. Carotenoids play a dual role in photoprotection, dissipating excess excitation energy via NPQ and scavenging ROS in chloroplasts, thereby protecting the photosynthetic apparatus under stress [61].

An integrated analysis of the results reveals that the physiological responses to Al and WD converge on a common axis of oxidative stress, which MeJA and cultivar background differentially modulate. Multivariate analyses highlighted strong associations among Al accumulation, lipid peroxidation, and proline concentration across all treatments (Figures 11–14), indicating that oxidative damage represents a central integrative outcome of stress integration rather than an isolated response. Reductions in leaf water potential under WD and $Al^{3+}$ stress promote stomatal closure, restricting $CO_2$ availability and limiting net photosynthetic rate and WUE [6]. Under these conditions, decreased photosynthetic activity increases excitation pressure on the photosynthetic apparatus, favoring ROS formation and lipid peroxidation, as widely reported for drought and $Al^{3+}$ stress [3,4,7–11].

In this context of oxidative stress, proline emerges as a key integrative metabolite. Beyond its classical role in osmotic adjustment, proline contributes to membrane stabilization, metal ion chelation, ROS scavenging, and the maintenance of cellular redox homeostasis [62,63]. The strong correlations between proline accumulation, Al concentration, and lipid peroxidation are therefore consistent with a multifunctional protective role of this amino acid under combined stress conditions. Non-enzymatic antioxidant responses also played a significant role in mitigating oxidative stress. Total phenolic compounds accumulated to a greater extent in the Al-sensitive cultivar Star, particularly in leaves, suggesting a compensatory response to elevated oxidative pressure (Figures 8–10). At the enzymatic level, antioxidant capacity emerged as a key determinant of stress tolerance. MeJA induced a differential activation of SOD, the antioxidant system, particularly in the cultivar Legacy, where SOD showed strong associations in multivariate analyses and inverse correlations with Al accumulation and lipid peroxidation (Figures 11–14). This differential activation of SOD, especially in Legacy, highlights the central role of jasmonates in mediating enzymatic antioxidant responses under abiotic stress. Previous studies have suggested that jasmonates not only induce the expression of antioxidant enzymes but also enhance resistance to oxidative damage by modulating hormonal signaling and cellular metabolism [20]. These patterns identify SOD as a robust marker of stress tolerance and reinforce the need to consider antioxidant capacity when selecting cultivars for abiotic stress conditions. In line with this interpretation, jasmonate-mediated enhancement of antioxidant enzyme activity has been reported in multiple species, including *Hordeum vulgare*, *Brasica napus*, and highbush blueberry, where increased SOD, APX, and GR activities were associated with reduced ROS accumulation and improved tolerance to drought, salinity, and metal toxicity [11,13,45,47]. Overall, these results indicate that MeJA reorganizes the oxidative stress response network by coordinating osmotic adjustment, non-enzymatic and enzymatic antioxidant defenses, and Al exclusion mechanisms. This coordinated regulation is more effective in the resistant cultivar Legacy, highlighting antioxidant capacity as a critical trait for stress resilience and cultivar selection under combined abiotic stress conditions.

## 5. Conclusions

In conclusion, this research demonstrates that highbush blueberry cultivars (*Vaccinium corymbosum*) exhibit highly differentiated physiological, biochemical, and hormonal responses to $Al^{3+}$ toxicity and WD, both individually and in combination. Exogenous application of MeJA played a central role in modulating defense responses and alleviating the effects of both individual and combined stresses. Its application reduces Al accumulation, maintains photosynthetic activity and auxin concentration, and increases protective amino acids such as Pro, with a more significant effect on the Al-resistant cultivar Legacy. The lower Al accumulation observed in Legacy may be associated with MeJA enhancement of WRKY-mediated regulation of the malate transporter ALMT. Such a mechanism could promote malate exudation into the rhizosphere and facilitate Al complexation, thereby

limiting its uptake by the plant; however, these potential mechanisms require further investigation to be fully elucidated in future studies. Furthermore, MeJA significantly reduced lipid peroxidation in both cultivars, although distinct mechanisms appear to operate between genotypes, with stronger enzymatic antioxidant responses in Legacy and enhanced non-enzymatic antioxidant responses in Star through increased phenolic compound accumulation. These results reinforce the role of MeJA as a key regulator of redox balance and an activator of metabolic pathways associated with abiotic stress tolerance. Taken together, these findings support the potential use of MeJA as a promising strategy to improve the physiological resilience of blueberries cultivated in acidic soils with Al availability and under scenarios of increasing water deficit.

## 6. Future Perspectives

Climate change has increased the frequency and severity of combined abiotic stresses, highlighting the need to elucidate the molecular mechanisms underlying tolerance to simultaneous Al toxicity and water deficit (Al + WD). Although physiological and biochemical responses to these individual stresses are well documented, substantial gaps remain in understanding the regulatory networks, stress-responsive proteins, and metabolic pathways underlying MeJA-induced resistance mechanisms. Comprehensive studies integrating proteomics, metabolomics, amino acid profiling, and physiological analyses are required to elucidate the coordinated molecular responses underlying combined-stress acclimation in blueberry plants.

On the other hand, future research should be directed towards elucidating whether MeJA regulates auxin homeostasis by activating tryptophan-dependent indole-3-acetic acid (IAA) biosynthesis pathways and modulating polar auxin transport under combined stress conditions. Particular attention should be given to the COI1–JAZ–MYC2 signaling cascade and its regulation of TAA1/TAR-, YUCCA-, AUX/LAX-, PIN-, and Aux/IAA-associated pathways involved in local auxin biosynthesis and signaling. Proteomic studies should also assess the activation of phenylpropanoid and flavonoid pathways via proteins such as PAL, C4H, CHS, F3H, and ANR, which may facilitate the detoxification of reactive oxygen species (ROS), membrane stabilization, and stress acclimation. Also, further proteomic investigations should examine how MeJA influences photosynthetic stability, oxidative stress responses, and stress-resistance mechanisms under combined aluminum and water deficit stress. Focus should be directed toward proteins involved in photosystem II (PSII) stability, electron transport, xanthophyll-cycle regulation, and antioxidant defense systems, including superoxide dismutase (SOD), ascorbate peroxidase (APX), glutathione S-transferase (GST), glutathione peroxidase (GPX), dehydroascorbate reductase (DHAR), thioredoxins, and glutaredoxins.

Further studies should determine whether MeJA enhances the accumulation of stress-associated proteins, such as late embryogenesis abundant (LEA) proteins, dehydrins, heat shock proteins (HSPs), molecular chaperones, and proteins involved in proteostasis and cellular protection. Integrating proteomic, physiological, and metabolic datasets may clarify the coordinated stress-resistance networks that contribute to redox balance, protein stabilization, photoprotection, and tolerance to combined aluminum and water-deficit stress. Thus, ongoing research into the molecular mechanisms underlying plant responses to combined WD-Al stress, with emphasis on protein function and advanced biotechnologies, is essential. Such efforts will facilitate the development of crop varieties with enhanced resistance to multiple abiotic stresses, thereby supporting global food security and sustainable agriculture.

**Supplementary Materials:** The following supporting information can be downloaded at: https://www.mdpi.com/article/10.3390/horticulturae12060728/s1. Figure S1: Experimental design and treatments.

**Author Contributions:** J.Q. and M.R.-D. conceptualized, designed, and coordinated the experiment; M.R.-D. supervised; M.R.-D. and C.S. obtained funding acquisition; J.Q., C.C., M.R.-D. and J.G.-V. carried out the physiological and biochemical analysis; J.Q. and C.C. performed the statistical analyses; J.Q., J.C. and M.R.-D. formulated the draft of the manuscript. J.Q., C.C., J.C., C.S., J.G.-V., C.I.-B., A.N.-N. and M.R.-D. revised and improved the current version of the manuscript. All authors have read and agreed to the published version of the manuscript.

**Funding:** This research was funded by the Agencia Nacional de Investigación y Desarrollo (ANID)/FONDECYT 1211856; ANID scholarship 21220322; ANID/ANILLO/ATE250064.

**Data Availability Statement:** The original contributions presented in this study are included in the article/Supplementary Materials. Further inquiries can be directed to the corresponding author.

**Acknowledgments:** We would like to thank Ximena Garrido, Jessica Yañez, and Mariela Mora for technical support. A.N.-N. thanks the Conselho Nacional de Desenvolvimento Científico e Tecnológico (CNPq-Brazil, and 406455/2022-8); and Foundation for Research Assistance of the Minas Gerais State (FAPEMIG-Brazil, grant RED 00060-23).

**Conflicts of Interest:** The authors declare no conflicts of interest.

## References

1. Garreaud, R.D.; Alvarez-Garreton, C.; Barichivich, J.; Boisier, J.P.; Christie, D.; Galleguillos, M.; Zambrano-Bigiarini, M. The 2010–2015 megadrought in central Chile: Impacts on regional hydroclimate and vegetation. *Hydrol. Earth Syst. Sci.* **2017**, *21*, 6307–6327. [CrossRef]
2. Xu, C.; Kohler, T.A.; Lenton, T.M.; Svenning, J.C.; Scheffer, M. Future of the human climate niche. *Proc. Natl. Acad. Sci. USA* **2021**, *117*, 11350–11355. [CrossRef] [PubMed]
3. Azam, A.; Hammad, A.; Javed, S.; Haq, S.A. Climate change and agricultural productivity: An economic assessment. *Food Agric. Comm.* **2025**, *2*, 49–54. [CrossRef]
4. Yang, X.; Lu, M.; Wang, Y.; Wang, Y.; Liu, Z.; Chen, S. Response mechanism of plants to drought stress. *Horticulture* **2021**, *7*, 50. [CrossRef]
5. Deligoz, A.; Gur, M. Morphological, physiological and biochemical responses to drought stress of Stone pine (*Pinus pinea* L.) seedlings. *Acta Physiol. Plant.* **2015**, *37*, 243. [CrossRef]
6. Zargar, S.; Gupta, N.; Nazir, M.; Mahajan, R.; Malik, F.A.; Sofi, N.R.; Shikari, A.B.; Salgotra, R.K. Impact of drought on photosynthesis: Molecular perspective. *Plant Gene* **2017**, *11*, 154–159. [CrossRef]
7. Kochian, L.V.; Piñeros, M.A.; Liu, J.; Magalhaes, J.V. Plant adaptation to acid soils: The molecular basis for crop aluminum resistance. *Ann. Rev. Plant Biol.* **2015**, *66*, 571–598. [CrossRef]
8. Bojórquez-Quintal, E.; Escalante-Magaña, C.; Echevarría-Machado, I.; Martínez-Estévez, M. Aluminum, a Friend or Foe of Higher Plants in Acid Soils. *Front. Plant Sci.* **2017**, *8*, 271596. [CrossRef]
9. Ofoe, R.; Thomas, R.H.; Asiedu, S.K.; Wang-Pruski, G.; Fofana, B.; Abbey, L. Aluminum in plant: Benefits, toxicity and tolerance mechanisms. *Front. Plant Sci.* **2023**, *13*, 1085998. [CrossRef] [PubMed]
10. Guo, C.; Shabala, S.; Chen, Z.-H.; Zhou, M.; Zhao, C. Aluminium tolerance and stomata operation: Towards optimising crop performance in acid soil. *Plant Physiol. Biochem.* **2024**, *210*, 108626. [CrossRef] [PubMed]
11. Ulloa-Inostroza, E.; Alberdi, M.; Ivanov, A.G.; Reyes-Díaz, M. Protective effect of methyl jasmonate on photosynthetic performance and its association with antioxidants in contrasting aluminum-resistant blueberry cultivars exposed to aluminum. *J. Soil Sci. Plant Nutr.* **2019**, *19*, 203–216. [CrossRef]
12. Butare, L.; Rao, I.; Lepoivre, P.; Polania, J.; Cajiao, C.; Cuasquer, J.; Beebe, S. New genetic sources of resistance in the genus Phaseolus to individual and combined aluminum toxicity and progressive soil drying stresses. *Euphytica* **2011**, *181*, 385–404. [CrossRef]
13. Reyes-Díaz, M.; Inostroza-Blancheteau, C.; Millaleo, R.; Cruces, E.; Wulff-Zottele, C.; Alberdi, M.; Mora, M.L. Long-term aluminum exposure effects on physiological and biochemical features of highbush blueberry cultivars. *J. Am. Soc. Hortic. Sci.* **2010**, *135*, 212–222. [CrossRef]

14. Bera, S.; De, A.K.; Adak, M.K. Modulation of glycine betaine accumulation with oxidative stress induced by aluminium toxicity in Rice. *Proc. Natl. Acad. Sci. India Sec. B—Biol. Sci.* **2019**, *89*, 291–301. [CrossRef]
15. Mishra, P.; Dubey, R.S. Effect of aluminium on metabolism of starch and sugars in growing rice seedlings. *Acta Physiol. Plant.* **2008**, *30*, 265–275. [CrossRef]
16. Ulloa-Inostroza, E.; Córdova, C.; Campos, M.; Reyes-Díaz, M. Methyl jasmonate application improves photosynthetic performance in blueberry plants under water deficit. *Horticulturae* **2024**, *10*, 259. [CrossRef]
17. Cáceres, C.; Cazor-Curilef, C.; Delgado-Santibañez, P.; González-Villagra, J.; Cárcamo-Fincheira, P.; Delgado, M.; Ribera-Fonseca, A.; Inostroza-BLanchetaeu, C.; Bravo, L.A.; Nunes-Nesi, A.; et al. Differential induction of resistance mechanisms by methyl jasmonate in two *Vaccinium corymbosum* L. cultivars under combined water deficit and aluminum toxicity. *Plants* **2025**, *14*, 3202. [CrossRef]
18. International Blueberry Organization-IBO. Global State of the Blueberry Industry Report. 2024. Available online: https://www.internationalblueberry.org/2024-report/ (accessed on 3 February 2026).
19. Cárcamo-Fincheira, P.; Reyes-Díaz, M.; Omena-García, R.P.; Vargas, J.R.; Alvear, M.; Florez-Sarasa, I.; Rosado-Souza, L.; Rengel, Z.; Fernie, A.R.; Nunes-Nesi, A.; et al. Metabolomic analyses of highbush blueberry (*Vaccinium corymbosum* L.) cultivars revealed mechanisms of resistance to aluminum toxicity. *Environ. Exp. Bot.* **2021**, *183*, 104338. [CrossRef]
20. Wang, Z.; Liu, L.; Su, H.; Guo, L.; Zhang, J.; Li, Y.; Xu, J.; Zhang, X.; Guo, Y.-D.; Zhang, N. Jasmonate and aluminum crosstalk in tomato: Identification and expression analysis of WRKYs and ALMTs during JA/Al-regulated root growth. *Plant Physiol. Biochem.* **2020**, *154*, 409–418. [CrossRef]
21. Gani, U.; Sharma, P.; Tiwari, H.; Nautiyal, A.K.; Kundan, M.; Wajid, M.A.; Kesari, R.; Nargotra, A.; Misra, P. Comprehensive genome-wide identification, characterization, and expression profiling of MATE gene family in *Nicotiana tabacum*. *Gene* **2021**, *783*, 145554. [CrossRef] [PubMed]
22. Đurić, M.; Subotić, A.; Prokić, L.; Trifunović-Momčilov, M.; Milošević, S. Foliar application of methyl jasmonate affects impatiens walleriana growth and leaf physiology under drought stress. *Plant Signal. Behav.* **2023**, *18*, e2219936. [CrossRef]
23. Khan, V.; Princi; Mubashshir, M.; Umar, S.; Iqbal, N. Methyl Jasmonate and Pseudomonas fluorescens synergistically boost antioxidative defense, secondary metabolites, and osmolyte production to enhance drought resilience in mustard. *J. Plant Growth Regul.* **2025**, *44*, 198–216. [CrossRef]
24. Lopes, A.S.; Dias, T.J.; Henschel, J.M.; da Silva, J.H.B.; de Oliveira Sousa, V.F.; Targino, V.A.; da Silva Leal, M.P.; da Silva Gomes, D.; de Albuquerque, M.B.; Batista, D.S. Methyl Jasmonate Mitigates Drought Stress in Purple Basil by Enhancing Photosynthesis and Secondary Metabolism. *J. Plant Growth Regul.* **2025**, *44*, 233–246. [CrossRef]
25. Mohamed, H.I.; Latif, H.H. Improvement of drought tolerance of soybean plants by using methyl jasmonate. *Physiol. Mol. Biol. Plants* **2017**, *23*, 545–556. [CrossRef]
26. Giné-Bordonaba, J.; Terry, L.A. Effect of deficit irrigation and methyl jasmonate application on the composition of strawberry (Fragaria x ananassa) fruit and leaves. *Sci. Hortic.* **2016**, *199*, 63–70. [CrossRef]
27. Cáceres, C.; Cazor-Curilef, C.; Delgado-Santibañez, P.; Machado, M.; Delgado, M.; Ribera-Fonseca, A.; Inostroza-Blancheteau, C.; Bravo, L.A.; González-Villagra, J.; Nunes-Nesi, A.; et al. Foliar Methyl Jasmonate Application Activates Antioxidant Mechanisms to Counteract Water Deficits and Aluminum Stress in *Vaccinium corymbosum* L. *Horticulturae* **2024**, *10*, 1172. [CrossRef]
28. Bryla, D.; Kaufman, D.; Strik, B. Effects of irrigation method and level of water application on fruit size and yield in red raspberry (*Rubus idaeus* L.) during the first year of full production. *HortScience* **2008**, *43*, 1112.
29. Almutairi, K.F.; Bryla, D.R.; Strik, B. Potential of deficit irrigation, irrigation cutoffs, and crop thinning to maintain yield and fruit quality with less water in northern highbush blueberry. *HortScience* **2017**, *52*, 625–633. [CrossRef]
30. Chen, X.; Qiu, L.; Guo, H.; Wang, Y.; Yuan, H.; Yan, D.; Zheng, B. Spermidine induces physiological and biochemical changes in southern highbush blueberry under drought stress. *Braz. J. Bot.* **2017**, *40*, 841–851. [CrossRef]
31. Slugeňová, K.; Ditmarová, L.; Kurjak, D.; Válka, J. Drought and aluminium as stress factors in Norway spruce (*Picea abies* [L.] Karst) seedlings. *J. For. Sci.* **2011**, *57*, 547–554. [CrossRef]
32. Sadzawka, A.; Grez, R.; Mora, M.L.; Saavedra, N.; Carrasco, M.A.; Rojas, C. Métodos de análisis de tejidos vegetales. Instituto de Investigaciones Agropecuarias (INIA), Santiago, Chile. *Ser. Actas INIA* **2007**, *40*, 72.
33. Hoffmann, W.; Poorter, H. Avoiding Bias in calculations of relative growth rate. *Ann. Bot.* **2002**, *90*, 37–42. [CrossRef]
34. Liu, X.; Hegeman, A.D.; Gardner, G.; Cohen, J.D. Protocol: High-throughput and quantitative assays of auxin and auxin precursors from minute tissue samples. *Plant Methods* **2012**, *8*, 31. [CrossRef]
35. Sarwar, M.; Kremer, R.J. Determination of bacterially derived auxins using a microplate method. *Lett. Appl. Microbiol.* **1995**, *20*, 282–285. [CrossRef]
36. Begg, J.E.; Turner, N.C. Water Potential Gradients in Field Tobacco. *Plant Physiol.* **1970**, *46*, 343–346. [CrossRef]
37. Rahimi, A.; Hosseini, S.M.; Rahimi, A.; Hosseini, S.M.; Pooryoosef, M.; Fateh, I. Variation of leaf water potential, relative water content and SPAD undergradual drought stress and stress recovery in two medicinal species of *Plantago ovata* and *P. psyllium*. *Plant Ecophysiol.* **2010**, *2*, 53–60.

38. Hatfield, J.L.; Dold, C. Water-use efficiency: Advances and challenges in a changing climate. *Front. Plant Sci.* **2019**, *10*, 103. [CrossRef]
39. García-Plazaola, J.I.; Becerril, J.M. A rapid high-performance liquid chromatography method to measure lipophilic antioxidants in stressed plants: Simultaneous determination of carotenoids and tocopherols. *Phytochem. Anal.* **1999**, *10*, 307–313. [CrossRef]
40. Hodges, D.M.; DeLong, J.M.; Forney, C.F.; Prange, R.K. Improving the thiobarbituric acid-reactive-substances assay for estimating lipid peroxidation in plant tissues containing anthocyanin and other interfering compounds. *Planta* **1999**, *207*, 604–611. [CrossRef]
41. Singleton, V.L.; Rossi, J.A. Colorimetry of total phenolics with phosphomolybdic-phosphotungstic acid reagents. *Am. J. Enol. Vitic.* **1965**, *16*, 144–158. [CrossRef]
42. Chinnici, F.; Bendini, A.; Gaiani, A.; Riponi, C. Radical scavenging activities of peels and pulps from cv. Golden Delicious apples as related to their phenolic composition. *J. Agric. Food Chem.* **2004**, *52*, 4684–4689. [CrossRef]
43. Giannopolitis, C.N.; Ries, S.K. Superoxide dismutases II. Purification and quantitative relationship with water-soluble protein in seedlings. *Plant Physiol.* **1977**, *59*, 315–318. [CrossRef]
44. Bradford, M.M. A rapid and sensitive method for the quantitation of microgram quantities of protein utilizing the principle of protein–dye binding. *Anal. Biochem.* **1976**, *72*, 248–254. [CrossRef]
45. Ahmed, I.M.; Nadira, U.A.; Qiu, C.W.; Cao, F.; Zhang, G.; Holford, P.; Wu, F. Tolerance to drought, low pH and Al combined stress in Tibetan wild barley is associated with improvement of ATPase and modulation of antioxidant defense system. *Int. J. Mol. Sci.* **2018**, *19*, 3553. [CrossRef]
46. Yang, Z.B.; Liu, G.; Liu, J.; Zhang, B.; Meng, W.; Müller, B.; Hayashi, K.I.; Zhang, X.; Zhao, Z.; De Smet, I.; et al. Synergistic action of auxin and cytokinin mediates aluminum-induced root growth inhibition in Arabidopsis. *EMBO Rep.* **2017**, *18*, 1213–1230. [CrossRef]
47. Pavlović, I.; Petřík, I.; Tarkowská, D.; Lepeduš, H.; Vujčić Bok, V.; Radić Brkanac, S.; Novák, O.; Salopek-Sondi, B. Correlations between phytohormones and drought tolerance in selected brassica crops: Chinese cabbage, white cabbage and kale. *Int. J. Mol. Sci.* **2018**, *19*, 2866. [CrossRef]
48. Liu, G.; Tian, H.; Wu, W.; Robert, H.S.; Ding, Z. Local transcriptional control of YUCCA regulates auxin-promoted root-growth inhibition in response to aluminum stress in *Arabidopsis thaliana*. *PLoS Genet.* **2016**, *12*, e1006360. [CrossRef]
49. Wang, H.; Wang, H.; Liu, H.; Wan, T.; Li, Y.; Zhang, K.; Shabala, S.; Li, X.; Chen, Y.; Yu, M. Aluminium stress-induced modulation of root gravitropism in pea (*Pisum sativum*) via auxin signalling. *Plant Physiol. Biochem.* **2024**, *206*, 108315. [CrossRef]
50. Chakraborty, N.; Das, A.; Pal, S.; Roy, S.; Sil, S.K.; Adak, M.K.; Hassanzamman, M. Exploring Aluminum Tolerance Mechanisms in Plants with Reference to Rice and Arabidopsis: A Comprehensive Review of Genetic, Metabolic, and Physiological Adaptations in Acidic Soils. *Plants* **2024**, *13*, 1760. [CrossRef]
51. Siecińska, J.; Wiącek, D.; Przysucha, B.; Nosalewicz, A. Drought in acid soil increases aluminum toxicity especially of the Al-sensitive wheat. *Environ. Exp. Bot.* **2019**, *165*, 185–195. [CrossRef]
52. Mohan, V.R.; MacDonald, M.T.; Abbey, L. Impact of Water Deficit Stress on Brassica Crops: Growth and Yield, Physiological and Biochemical Responses. *Plants* **2025**, *14*, 1942. [CrossRef]
53. Yang, X.; Rao, I.M.; Horst, W.J. Interaction of aluminum and drought stress on root growth and crop yield on acid soils. *Plant Soil* **2013**, *372*, 3–25. [CrossRef]
54. Masheva, V.; Spasova-Apostolva, V.; Aziz, S.; Tomlekova, N. Variations in proline accumulation and relative water content under water stress characterize bean mutant lines (*P. vulgaris* L.). *Bulg. J. Agric. Sci.* **2022**, *28*, 430–436.
55. Zhang, X.; Wang, Z.; Li, Y.; Guo, R.; Liu, E.; Liu, X.; Gu, F.; Yang, Z.; Li, S.; Zhong, X.; et al. Wheat genotypes with higher yield sensitivity to drought overproduced proline and lost minor biomass under severer water stress. *Front. Plant Sci.* **2022**, *13*, 1035038. [CrossRef]
56. Khan, P.; Abdelbacki, A.M.M.; Albaqami, M.; Jan, R.; Kim, K.-M. Proline Promotes Drought Tolerance in Maize. *Biology* **2025**, *14*, 41. [CrossRef]
57. Munemasa, S.; Mori, I.C.; Murata, Y. Methyl jasmonate signaling and signal crosstalk between methyl jasmonate and abscisic acid in guard cells. *Plant Signal Behav.* **2011**, *6*, 939–941. [CrossRef]
58. Phutela, A.; Jain, V.; Dhawan, K.; Nainawatee, H.S. Proline Metabolism Under Water Stress in the Leaves and Roots of *Brassica juncea* Cultivars Differing in Drought Tolerance. *J. Plant Biochem. Biotech.* **2012**, *9*, 35–39. [CrossRef]
59. Allagulova, C.; Avalbaev, A.; Fedorova, K.; Shakirova, F. Methyl jasmonate alleviates water stress-induced damages by promoting dehydrins accumulation in wheat plants. *Plant Physiol. Biochem.* **2020**, *155*, 676–682. [CrossRef]
60. Sonatan, S.D.; Paul, J.K.; Azmal, M.; Haque, A.S.N.B.; Ghosh, A. The role of jasmonic acid and methyl jasmonate in enhancing photosynthesis and stress response. *J. Plant Physiol.* **2026**, *318*, 154725. [CrossRef]
61. Demmig-Adams, B.; Hodges, A.K.; Polutchko, S.K.; Adams, W.W., III. Zeaxanthin and Other Carotenoids: Roles in Abiotic Stress Defense with Implications for Biotic Defense. *Plants* **2025**, *14*, 2703. [CrossRef] [PubMed]

62. Hildebrandt, T.M.; Nunes Nesi, A.; Araújo, W.L.; Braun, H.P. Amino acid catabolism in plants. *Mol. Plant* **2015**, *8*, 1563–1579. [CrossRef] [PubMed]
63. Liang, X.; Zhang, L.; Natarajan, S.K.; Becker, D.F. Proline mechanisms of stress survival. *Antioxid. Redox Signal.* **2013**, *19*, 998–1011. [CrossRef]